

See discussions, stats, and author profiles for this publication at: <https://www.researchgate.net/publication/317568775>

Systematic revision of *Acanthodactylus busacki* (Squamata: Lacertidae) with a description of a new species from Morocco

Article in *Zootaxa* · June 2017

DOI: 10.11646/zootaxa.4276.3.3

CITATIONS

0

READS

53

4 authors, including:



Karin Tamar

Tel Aviv University

24 PUBLICATIONS 32 CITATIONS

[SEE PROFILE](#)



José Carlos Brito

CIBIO Research Center in Biodiversity and Ge...

313 PUBLICATIONS 2,333 CITATIONS

[SEE PROFILE](#)



Pierre-André Crochet

French National Centre for Scientific Research

295 PUBLICATIONS 2,587 CITATIONS

[SEE PROFILE](#)

Some of the authors of this publication are also working on these related projects:



Evolutionary ecology of desert organisms [View project](#)



Mohammed bin Zayed Species Conservation Fund to CGV (11052707) [View project](#)



<https://doi.org/10.11646/zootaxa.4276.3.3>

<http://zoobank.org/urn:lsid:zoobank.org:pub:CB669212-EF39-4D3B-9B87-C729FEC2E15C>

Systematic revision of *Acanthodactylus busacki* (Squamata: Lacertidae) with a description of a new species from Morocco

KARIN TAMAR^{1,2,6}, PHILIPPE GENIEZ³, JOSÉ C. BRITO⁴ & PIERRE-ANDRÉ CROCHET⁵

¹The Steinhardt Museum of Natural History, Israel National Center for Biodiversity Studies, Tel Aviv University, 6997801 Tel-Aviv, Israel

²Department of Zoology, George S. Wise Faculty of Life Sciences, Tel Aviv University, 6997801 Tel Aviv, Israel

³EPHE, PSL Research University, CNRS, UM, SupAgro, IRD, INRA, UMR 5175 Centre d'Écologie Fonctionnelle et Évolutive (CEFE), F-34293 Montpellier cedex 5, France

⁴CIBIO/InBIO, Centro de Investigação em Biodiversidade e Recursos Genéticos da Universidade do Porto, R. Padre Armando Quintas, 4485-661 Vairão, Portugal

⁵CEFE UMR 5175, CNRS - Université de Montpellier - Université Paul-Valéry Montpellier - EPHE, 1919 Route de Mende, 34293 Montpellier cedex 5, France

⁶Corresponding author. E-mail: karintmr@gmail.com

Abstract

Recent molecular phylogenies of the *Acanthodactylus pardalis* species-group have revealed a deep genetic divergence within the nominal species *A. busacki* from north-west Africa. The species is phylogenetically separated into northern and southern lineages, which correspond to a previously observed morphological differentiation between the northern and southern populations of this species. Based on morphological comparisons of the type material and location of the type locality, the nomen *Acanthodactylus busacki* Salvador, 1982 is assigned here to the southern lineage, known from the northern Saharan Atlantic coastal desert. The northern lineage, described here as *Acanthodactylus margaritae* sp. nov., is prominently characterized by weakly keeled dorsal scales and a characteristic colour pattern. The new species is endemic to Morocco and confined to arid and semi-arid bioclimatic areas between the High Atlas and Anti-Atlas Mountains, from around Tamri in the north to Tiznit in the south and the Souss valley in the east.

Key words: Atlas Mountains, evolution, lizards, *pardalis* species-group, phylogeny, taxonomy

Introduction

The Old World lacertid lizards of the genus *Acanthodactylus* Fitzinger, 1834 comprise over 40 currently recognized species (Uetz & Hošek 2017). *Acanthodactylus* are diurnal, ground-dwelling, medium-sized lizards, occurring mostly in xeric habitats in North Africa and south-west Asia (Salvador 1982; Arnold 1983; Sindaco & Jeremčenko 2008). The genus has been divided into several species-groups based on overall morphological similarities and scant genetic data, although the boundaries of species and species-groups and the relationships among them are often unclear and controversial (Salvador 1982; Arnold 1983; Harris & Arnold 2000; Crochet *et al.* 2003; Harris *et al.* 2004; Fonseca *et al.* 2008, 2009; Tamar *et al.* 2014, 2016).

The *Acanthodactylus pardalis* species-group currently comprises seven species, mostly distributed in the northern and western areas of North Africa, with two localised species in southern Israel and in Jordan (Salvador 1982; Arnold 1983; Schleich *et al.* 1996; Sindaco & Jeremčenko 2008; Tamar *et al.* 2016). This species-group is an interesting example of confusing systematics as the current species-level classification clearly does not reflect evolutionary relationships, as evidenced by recent genetic data on the complex (Fonseca *et al.* 2008; Tamar *et al.* 2016). Those two studies recovered multiple non-monophyletic “species” and geographic clustering of specimens independently of species assignment, underlining the need for a thorough systematic revision with the probable detection of several currently undescribed taxa.

Within the *pardalis* species-group, *Acanthodactylus busacki* Salvador, 1982 was described from 30 km south

of Goulimine (= Guelmim, Morocco). Other specimens from along the Atlantic coast between Tamri and Cape Bojador (Boujdour) were assigned to the species, as well as specimens from north-eastern Morocco (Itzer, Mahiridja, Taourirt, Ain Guattara; Salvador 1982). The distribution was later extended to adjacent south-western Algeria (Tindouf region) by Donaire *et al.* (2000, but see below for discussion of these records). However, recent studies have restricted the range of *A. busacki* to the Atlantic coast alone, assigning the populations from north-eastern Morocco to the morphologically similar species *A. maculatus* (Bons & Geniez 1996; Schleich *et al.* 1996; Fonseca *et al.* 2008; Sindaco & Jeremčenko 2008; Trape *et al.* 2012; Tamar *et al.* 2016). Geniez *et al.* (2004), followed by Brito *et al.* (2008), noted that *A. busacki* has a very variable colouration, as the northern and southern populations of this species exhibit a different colouration (lineated *vs.* marbled dorsal pattern), calling for further investigation. These observations are in accordance with the results of recent phylogenetic studies of the *pardalis* species-group based on mitochondrial data (Fonseca *et al.* 2008) and of the entire genus based on both mitochondrial and nuclear data (Tamar *et al.* 2016). Samples of *A. busacki* were separated into two distinct lineages within its known distribution range—a northern lineage from the arid and semi-arid bioclimatic areas between the High Atlas and Anti-Atlas Mountains, and a southern lineage from the northern Saharan Atlantic coastal desert.

The genetic and phenotypic division of *A. busacki* and its confusing morphology necessitate a more thorough study of its nomenclatural status, taxonomy and distribution. In this study, we use morphological as well as mitochondrial and nuclear molecular data to further explore the systematics of *A. busacki*. Our analyses confirm a distinction between two groups: the northern populations are described herein as a new species, endemic to Morocco.

Materials and methods

Taxon sampling, DNA extraction and sequence analysis. In order to resolve the phylogenetic relationships between the two lineages of *A. busacki* within the *pardalis* species-group, 14 individuals of *A. busacki* were included in the molecular study (sequences of nine specimens were retrieved from GenBank). Other sequences of the *pardalis* species-group were retrieved from GenBank (from the study of Tamar *et al.* 2016), with the addition of four newly-sequenced individuals of *A. maculatus*. Two specimens of *A. erythrurus* were used to root the tree based on published evidence (Fonseca *et al.* 2008; Tamar *et al.* 2016). A list of all *A. busacki* (*sensu lato*) individuals included in the molecular analyses, together with their taxonomic identifications, voucher codes, localities, and GenBank accession codes is presented in Table 1. Localities are shown in Fig. 1. The other *pardalis* species-group members included in the molecular analyses, with their GenBank accession codes and localities, are listed in Appendix I (including outgroups).

Genomic DNA was extracted from ethanol-preserved tissue samples using the Qiagen DNeasy Blood & Tissue Kit (Qiagen, Valencia, CA, USA). All individuals were sequenced for two mitochondrial gene fragments, a portion of the ribosomal 12S rRNA (*12S*) gene and of the cytochrome *b* (*cytb*) gene, and three nuclear gene fragments from the melano-cortin 1 receptor (*MC1R*) gene, from the acetylcholinergic receptor M4 (*ACM4*) gene, and from the oocyte maturation factor MOS (*c-mos*) gene. Gene fragments were amplified and sequenced for both strands. Primers and PCR conditions for the amplification of all fragments are the same as listed in Table S2 in Tamar *et al.* (2016).

Chromatographs were checked manually, assembled and edited using Geneious v.7.1.9 (Biomatter Ltd.). For the nuclear gene fragments (*MC1R*, *ACM4*, *c-mos*) heterozygote positions were identified and coded according to the IUPAC ambiguity codes. Coding gene fragments (*cytb*, *MC1R*, *ACM4*, *c-mos*) were translated into amino acids to validate the correct reading frame and no stop codons were observed, suggesting that the sequences were all functional. DNA sequences were aligned for each gene independently using the online version of MAFFT v.7.3 (Katoh & Standley 2013) with default parameters. For the *12S* fragments we applied the Q-INS-i strategy in which data on the secondary structure of the RNA are considered. Poorly aligned positions of *12S* were eliminated with Gblocks (Castresana 2000) using less stringency options (Talavera & Castresana 2007). Inter and intra-specific uncorrected *p*-distances and the number of variable (*V*) and parsimony informative (*Pi*) sites were calculated in MEGA v.7 (Kumar *et al.* 2016).

Phylogenetic analyses and nuclear networks. The best-fit partitioning scheme and models of molecular evolution were selected using PartitionFinder v.2.1.1 (Lanfear *et al.* 2016) with the following parameters: linked

branch lengths; best models of evolution; BIC model selection; all search schemes; five data blocks (one for each of the five gene fragments). The complete concatenated dataset of the *pardalis* species-group comprised the following partition scheme (and selected model of sequence evolution): *12S* (HKY+I); *cytb* (HKY+G); *MC1R+ACM4+c-mos* (K80+I+G).

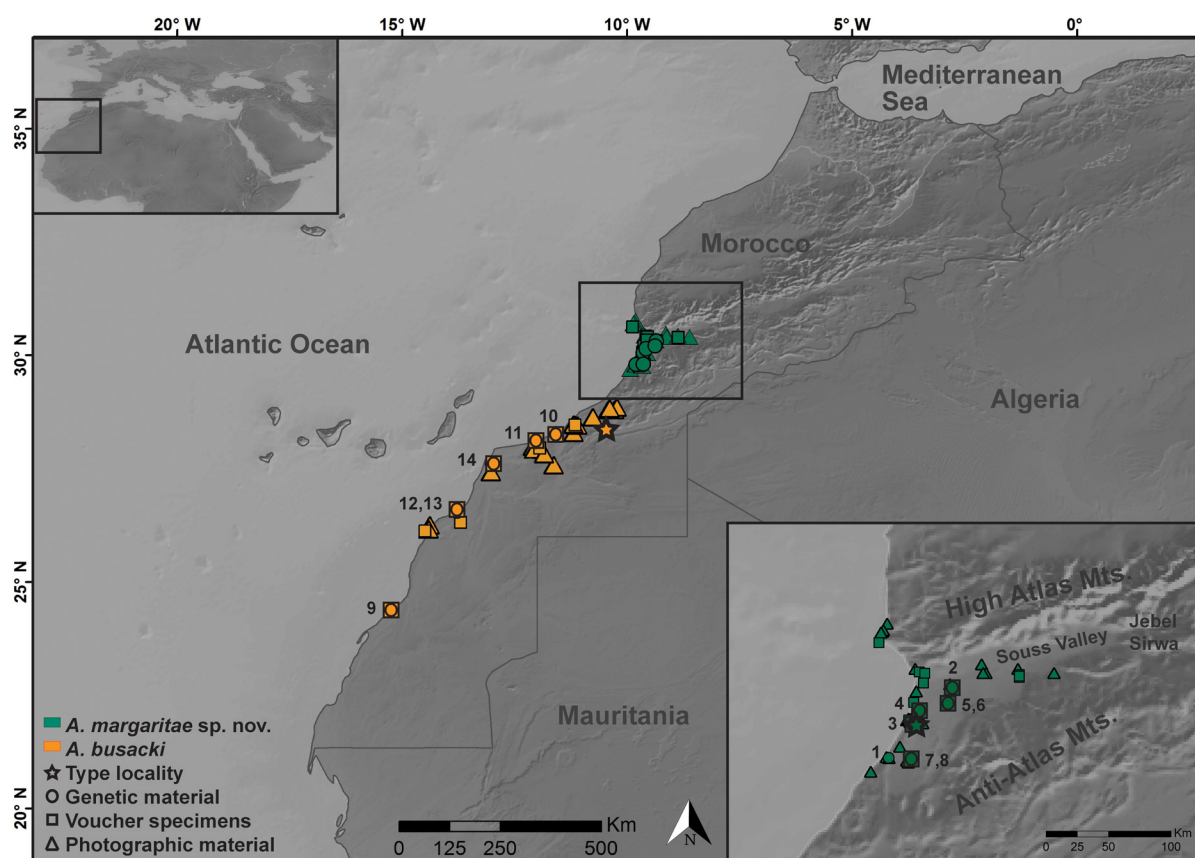


FIGURE 1. Localities of the material examined in this study for *Acanthodactylus margaritae* sp. nov. (green symbols) and *A. busacki* (orange symbols), with type localities (star), samples used for the genetic analyses (circle), voucher specimens (square), and photographic material (triangle). Numbers correspond to samples listed in Table 1. Taxon names correspond to changes proposed in this paper.

Phylogenetic analyses were performed on the partitioned complete concatenated dataset (as specified above) using maximum likelihood (ML) and Bayesian inference (BI) methods. We treated alignment gaps as missing data, and the nuclear gene sequences were not phased. Maximum likelihood analyses were performed with RAxML v.7.4.2 (Stamatakis 2006) as implemented in raxmlGUI v.1.3 (Silvestro & Michalak 2012). The ML analyses were performed with the GTR+G model of evolution and 100 replicates. Each inference was initiated with a random starting tree and nodal support was assessed with 1000 bootstrap pseudoreplicates (Stamatakis *et al.* 2008). Bayesian inference analyses were performed with BEAST v.1.8.2 (Drummond *et al.* 2012). Three individual runs were performed for 7×10^7 generations with a sampling frequency of 7000. We tested if the genes evolved in a clock-like manner using a likelihood ratio test (LRT) implemented in MEGA. The clock-like evolution of all genes was not rejected at a 5% significance level, thus a strict clock prior was selected. The following models and prior specifications were applied, otherwise by default: parameter values both for clock and substitution models unlinked across partitions, trees linked; models of sequence evolution for the different partitions as selected by PartitionFinder (see above); Yule process of speciation tree prior; random starting tree; strict clock; molecular clock model (rate fixed at 1); Alpha prior Uniform (0, 10); clock.rate prior Uniform (0, 1). The “useAmbiguities” parameter in the .xml file was manually modified to “true” for the nuclear partition (*MC1R+ACM4+c-mos*) to account for variability in the heterozygote positions, rather than treating them as missing data. Convergence of runs was assessed through the effective sample size values of parameters (>200) using Tracer v.1.6 (Rambaut *et al.* 2014). LogCombiner and TreeAnnotator (both available in BEAST package) were used to produce the ultrametric

tree after discarding 10% as burn-in. Nodes were considered strongly supported if they received ML bootstrap values $\geq 70\%$ and posterior probability (pp) support values ≥ 0.95 (Wilcox *et al.* 2002; Huelsenbeck & Rannala 2004).

Nuclear haplotype networks were constructed to infer genealogical relationships for the *A. busacki* dataset alone (Table 1). We used SEQPHASE (Flot 2010) to convert the input files, and the software PHASE v.2.1.1 (Stephens *et al.* 2001; Stephens & Scheet 2005) to resolve phased haplotypes. Default settings of PHASE were used except for phase probabilities that were set as ≥ 0.5 . The phased nuclear sequences were used to generate median-joining networks using NETWORKS v.5 (Bandelt *et al.* 1999). Genetic differentiation between lineages for each phased nuclear marker was estimated via Wright's *F_{st}* using DnaSP v.5.10.01 (Librado & Rozas 2009).

Morphological dataset and museums acronyms. Material for the morphological analyses of *A. busacki* comprised specimens from most of the known north-western distribution of the *pardalis* species-group (i.e., from Morocco and from the northern Saharan Atlantic coastal desert). We examined 67 alcohol-preserved specimens identified as *Acanthodactylus busacki* (these specimens comprise almost all the material examined by Salvador 1982, including the specimens later classified as *A. maculatus*). In addition, 26 voucher specimens, including the holotype of *Acanthodactylus busacki* (BMNH1970.250), and 54 live individuals were examined from photographs; they were used for meristic and colouration characters, but not measured. A list of all examined specimens with their localities is presented in Appendix II. The material studied was obtained from the following collections: [BEV] Biogéographie et Écologie des Vertébrés, Centre d'Écologie Fonctionnelle et Évolutive, Montpellier, France; [BMNH] Natural History Museum, London, UK; [CAS] California Academy of Sciences, San Francisco, USA; [FMNH] Field Museum of Natural History, Chicago, USA; [MB] Museu Nacional de História Natural e da Ciência (MUHNAC), Lisbon, Portugal; [MCCI-R] Museo Civico di Storia Naturale, Carmagnola, Turin, Italy; [MNHN] Muséum national d'Histoire naturelle, Paris, France; [PGe] Photo collection of Philippe Geniez, Montpellier, France; [ZFMK] Zoologisches Forschungsmuseum Alexander Koenig, Bonn, Germany; [ZMH] Zoologisches Museum Hamburg, Germany.

Morphological characters. Characters for the morphological analyses were selected based on previous taxonomic studies of *Acanthodactylus busacki* (Salvador 1982; Arnold 1983) and on personal observations. The following mensural characters were taken by the first author (K.T.) on the left side of each specimen (if bilateral) using a Helios calliper with accuracy to the nearest 0.1 millimetre (mm): snout-vent length (SVL); head length (HL; tip of snout to posterior margin of parietals); head width (HW; largest distance between outer margins of the supratemporals); head height (HH); forelimb length (ForeL; from axilla to tip of distal claw); hindlimb length (HindL; from groin to tip of distal claw); tail length (TailL; measured from cloaca to tip of original tail only).

The following meristic characters were examined under a stereomicroscope: number of longitudinal rows of dorsal scales at mid-body (Dors); number of transversal rows of ventral plates (Vent); number of gular scales in a longitudinal direction (Gul); number of collar scales (Collar); number of femoral pores on each side (Fpor L/R); number of lamellae under fourth toe (Lame); number of supraocular granules rows (Gran); total number of granules around the supraoculars on each side (Supraoc L/R); number of transverse temporal scales in a longitudinal direction on each side (Temp L/R).

Four ordinal meristic characters describing degree of carination and contact of femoral pores rows (not modified in preserved specimens) were: shape of the upper and lower temporal scales (smooth/weakly carinated/well carinated); carination of the dorsal scales (smooth/weakly carinated/well carinated); contact of the femoral pores rows (yes/no).

Five colouration characters, describing colour patterns (the latter two are visible on live specimens or photographs only, as they disappear in preservation) were: presence/absence of longitudinal dorsal white lines or rows of ocelli; number of longitudinal dorsal white lines or rows of ocelli; presence/absence of dorsal black reticulation at midbody; dorsal colour change; ventral tail colour (white/reddish/blue).

Statistical analyses. The seven mensural, nine meristic, and four ordinal characters were analysed independently, and the five colouration characters were described separately. The datasets for each character set are listed in Table 2.

As the database of the southern lineage of *A. busacki* features a low sample size of females with an incomplete dataset of variables, we cannot provide comparisons for females. Therefore, our comparisons were restricted to males of the northern and southern assemblages. Taxonomic differences between the males of the two lineages were tested using one-way ANOVA for the meristic variables (including data from specimens of all ages), and the

mensural traits were tested using one-way ANCOVA (SVL as a covariate for size correction; \log_{10} -transformed before the analyses; adult specimens only). We performed the Bonferroni correction for multiple testing and present the results that were found significant after this correction. Ordinal characters were tested using the Fisher's exact probability test. The different datasets were tested for normality using the Shapiro-Wilk's test and homogeneity of variances using the Leven's test. All analyses were performed in IBM SPSS Statistics 23 (IBM Corp. Armonk, NY). Sexual dimorphism could only be examined for the northern lineage, which has a proper sampling of both males and females, and was tested as described above.

Results

Molecular analyses. The dataset used for the phylogenetic analyses comprised 51 specimens of *Acanthodactylus*: six of *A. busacki sensu stricto*, eight of the new species described herein, 35 of the other *pardalis* species-group members, and two of *A. erythrurus* that were used as outgroup. The dataset of 2405 bp comprised mitochondrial gene fragments of *12S* (386 bp; $V=72$; $Pi=64$) and *cytb* (405 bp; $V=150$; $Pi=134$), and nuclear gene fragments of *MC1R* (663 bp; $V=24$; $Pi=14$), *ACM4* (429 bp; $V=18$; $Pi=6$), and *c-mos* (522 bp; $V=20$; $Pi=12$).

The concatenated trees of the *pardalis* species-group were almost identical for both the ML and BI methods, and recovered nine clades with distinct geographical origins. The two methods only differed to some extent in the phylogenetic positions of the deeper, less supported nodes, where the topology varied between the trees (Fig. 2; Appendix III). The *A. busacki (sensu lato)* samples are phylogenetically monophyletic, though this topology is not supported in either the ML or BI methods (ML: 30%; BI: 0.67), and form two well-supported clades: a southern clade from the northern Saharan Atlantic coastal desert (orange symbols in Fig. 1) and a northern clade from the arid and semi-arid bioclimatic areas between the High Atlas and Anti-Atlas Mountains (green symbols in Fig. 1). The uncorrected genetic divergences (p -distances) between the two *A. busacki* clades are 5.7% for *12S* and 12.6% for *cytb*. The level of genetic variability within the southern clade is 0.3% (*12S*) and 0.2% (*cytb*), and within the northern clade 0.5% (*12S*) and 1.2% (*cytb*).

The results of the nuclear networks of *A. busacki (sensu lato)* are presented in Fig. 3. The three nuclear networks show obvious differences in allele frequency between the northern and the southern clades in spite of extensive allele sharing. Dedicated analyses of gene flow with a higher number of markers would be needed to test for recent gene flow between the two lineages. A high level of genetic differentiation ($F_{st}=0.427$ and 0.482 for *MC1R* and *c-mos*, respectively) was found between the northern and southern lineages, and less for *ACM4* ($F_{st}=0.204$).

Morphological examinations and analyses. The morphological dataset comprised 49 voucher specimens, and photographs of 21 additional voucher specimens and of 54 live specimens of *A. busacki (sensu lato)* (38, 19, and 29 of which, respectively, belong to the northern clade described as a new species herein), and 18 voucher specimens and five photographs of voucher specimens of *A. cf. maculatus* (Appendix II). The database comprised seven mensural, nine meristic, four ordinal, and five colouration characters. Descriptive statistics for all 25 variables included in the morphological examinations are presented in Table 2.

The results of the sexual dimorphism analysis within the northern lineage did not detect significant differences for most of the mensural or meristic variables ($P>0.07$ for all variables). Sexual differences were significant for the number of femoral pores, for which males have a higher count (Fpor; $F=23.589$, 31.631; d.f.=40, 44; $P<0.0001$ for the left and right sides, respectively).

Statistical tests did not detect significant differences between males of the two clades for the mensural traits ($P>0.16$ for all variables) and for eight meristic variables ($P>0.07$ for Dors, Vent, Gul, FporL, Lame, Gran, Temp L/R). Significant differences were found for four characters indicating that the northern clade has a higher number of granules around the supraoculars (Supraoc; $F=21.248$, 18.615; d.f.=1, 40; $P<0.0001$ for the left and right sides, respectively) and of collar scales (Collar; $F=24.260$; d.f.=1, 28; $P<0.0001$), but the number of femoral pores on the right side is relatively higher in the southern clade (FporR; $F=9.993$; d.f.=1, 34; $P=0.017$).

The analyses of the ordinal characters show that the northern and southern clades share the same characteristics regarding the shape of the upper and lower temporal scales. Both assemblages present granular upper temporals and smooth lower temporals. The analysis of the contact between the femoral pores rows shows that for both clades females present 100% separation (usually by more than one scale), while males present contact

in 89% and 83% of the specimens, for the northern and southern clades, respectively. The results of the Fisher's exact probability test on this variable show significant sexual dimorphism ($P < 0.0001$) for both assemblages. The shape and carination of the dorsal scales show two distinct states, weakly carinated and smooth, with a clear difference between the two clades (Fig. 4). All specimens of the northern clade have weakly carinated, flat and imbricate dorsal scales, while the southern ones exhibit smooth and pointed/granular scales.

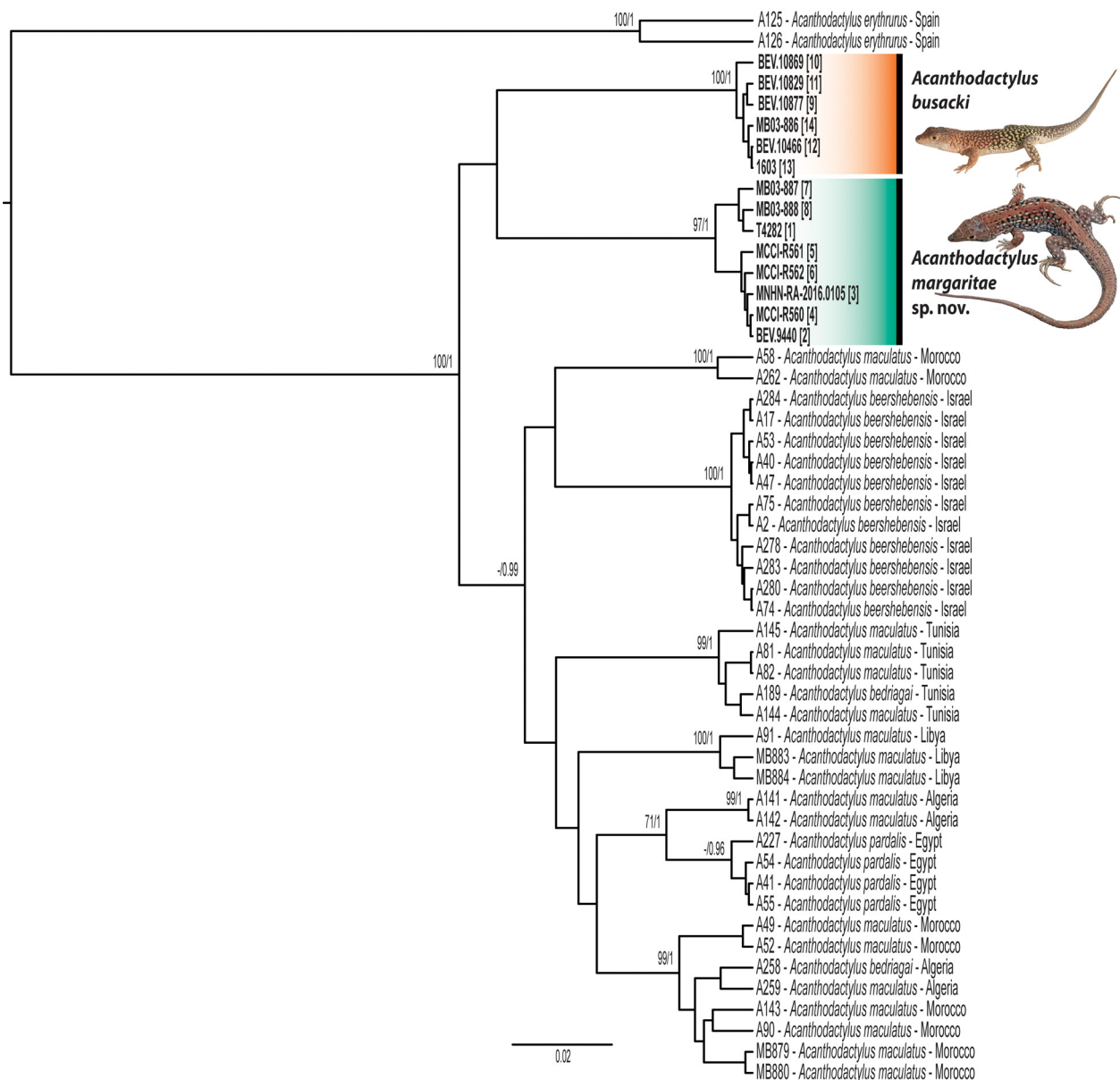


FIGURE 2. Bayesian inference phylogenetic tree of the *pardalis* species-group reconstructed from 2405 bp of mitochondrial (*12S*, *cytb*) and nuclear (*MC1R*, *ACM4*, *c-mos*) gene fragments. Bootstrap and posterior probabilities values are presented near the nodes (ML/BI; values $\geq 70\%$ and ≥ 0.95 , respectively). Taxon names correspond to changes proposed in this paper.

Colouration of the two clades presents differences of sex and age (Fig. 5):

(i) Dorsal colour pattern. The northern clade, for both males and females, exhibits three longitudinal white lines/rows of ocelli on each side, with black reticulation between them; dark dorsal reticulation is almost always absent on the middle of the dorsum. In contrast, the southern lineage has two longitudinal white lines/rows of ocelli with obvious black reticulation among them; the dark reticulation is prominent also on the middle of the dorsum. Males of the southern clade often exhibit a very strong, intricate black reticulation with the longitudinal white lines of ocelli often almost undistinguishable.

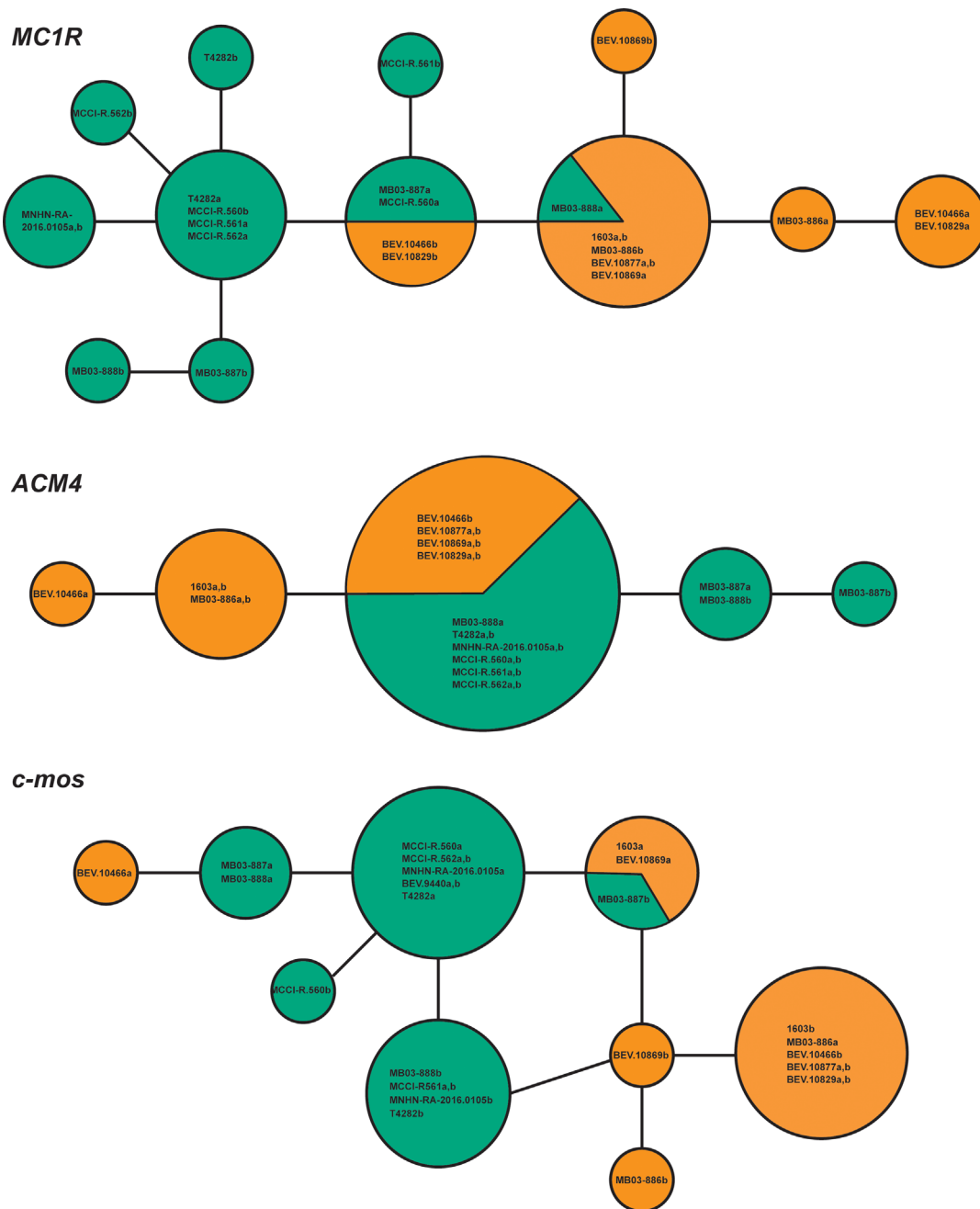


FIGURE 3. Unrooted networks of the phased nuclear markers (*MC1R*, *ACM4*, *c-mos*). Circle size is proportional to the number of alleles, with colours corresponding to species in Figs. 1 & 2. Codes correlate to the two alleles (i.e., a and b) of specimens listed in Table 1.

(ii) Head and dorsal colour. The northern clade's head and dorsal colouration is yellowish to white for both males and females, and the ground colour is not clearly differentiated between the anterior and posterior parts of the animals, even in males. The yellowish (pure yellow in males in courtship colours) colouration is most prominent during the months of February–April and weakens or disappears during the summer. In the southern clade males exhibit a reddish dorsal colouration at the nape changing to yellow and white/bluish at the tail. In old males, this reddish colouration extends beneath the throat and the anterior part of the belly.

(iii) Ventral tail colouration. Similarly between the two species, adult females and sub-adults of both sexes have reddish or whitish ventral tail colour. Juveniles of the northern clade and juveniles of the northern populations of the southern clade have blue tail colouration. Due to the lack of juvenile specimens from the southern populations of the southern clade, we cannot provide colouration data for this age group.

TABLE 1. Data on *Acanthodactylus margaritae* sp. nov. and *A. busacki* specimens used in the genetic analyses and their GenBank accession codes. Localities are presented in Fig. 1. Taxon names correspond to changes proposed in this study.

Locality	Sample code*	Specimen Voucher	Species	Latitude	Longitude	IZS	cyb	MCIR	ACM4	c-mos
1	BEV.T4282 (PGe.1174) BEV.9440	---	<i>A. margaritae</i> sp. nov.	29.8012	-9.8097	KX296968	KX297170	KX297348	KX297430	KX297626
2	BEV.9440	BEV.9440	<i>A. margaritae</i> sp. nov.	30.3157	-9.3600	KX296969	KX297171	-	-	KX297630
3	MNHN-RA- 2016.0105	MNHN-RA- 2016.0105	<i>A. margaritae</i> sp. nov.	30.0580	-9.6456	KX296970	KX297172	KX297349	KX297434	KX297627
4	MCCI-R560	MCCI-R560	<i>A. margaritae</i> sp. nov.	30.1500	-9.5900	KX296971	KX297173	KX297336	KX297435	KX297636
5	MCCI-R561	MCCI-R561	<i>A. margaritae</i> sp. nov.	30.2100	-9.3800	KX296972	KX297174	KX297337	KX297436	KX297629
6	MCCI-R562	MCCI-R562	<i>A. margaritae</i> sp. nov.	30.2100	-9.3800	KX296973	KX297175	KX297350	KX297437	KX297624
7	MB03-887	MB03-887	<i>A. margaritae</i> sp. nov.	29.8061	-9.6475	KY807721	KY807730	KY807739	KY807748	KY807756
8	MB03-888	MB03-888	<i>A. margaritae</i> sp. nov.	29.8061	-9.6475	KY807722	KY807731	KY807740	KY807747	KY807755
9	BEV.10877	BEV.10877	<i>A. busacki</i>	24.3898	-15.2494	KX296965	KX297167	KX297338	KX297431	KX297644
10	BEV.10869	BEV.10869	<i>A. busacki</i>	28.2656	-11.5908	KX296967	KX297168	KX297339	KX297432	KX297646
11	BEV.10829	BEV.10829	<i>A. busacki</i>	28.1001	-12.0389	KX296966	KX297169	KX297332	KX297433	KX297645
12	BEV.10466	BEV.10466	<i>A. busacki</i>	26.5671	-13.7923	KY807718	KY807727	KY807736	KY807744	KY807752
13	Brito1603	---	<i>A. busacki</i>	26.5671	-13.7923	KY807719	KY807728	KY807737	KY807745	KY807753
14	MB03-886	MB03-886	<i>A. busacki</i>	27.5956	-12.9983	KY807720	KY807729	KY807738	KY807746	KY807754

Sample code abbreviations: [BEV] Biogéographie et Écologie des Vertébrés, Centre d'Écologie Fonctionnelle et Évolutive, Montpellier, France; [Brito] Private collection José C. Brito, Portugal; [MB] Museu Nacional de História Natural e da Ciência (MUHNAC), Lisbon, Portugal; [MCCI-R] Museo Civico di Storia Naturale, Carmagnola, Turin, Italy; [MNHN] Muséum national d'Histoire naturelle, Paris, France.

TABLE 2. Morphological variables of *Acanthodactylus margaritae* sp. nov. and *A. busacki*. Mean ± standard deviation, range (parentheses) and sample size (brackets) are given. Mensural variables were taken from adult specimens only and are presented in millimetres. Variable abbreviations are listed in the Materials and Methods section. Taxon names follow the taxonomy recommended in this study.

Variable	<i>A. margaritae</i> sp. nov.		<i>A. busacki</i>	
	Males	Females	Males	Females
SVL	63.8±5.8 (54–71) [n=12]	60.2±3.8 (54–64.7) [n=14]	61.9±8.6 (51–73) [n=7]	---
TailL	107.6±15.3 (87–130.9) [n=8]	91.6±13.4 (74.5–115) [n=9]	97.3±6.8 (91–105) [n=4]	---
HL	15.3±1.4 (12.8–17.1) [n=7]	14±0.9 (12.5–15.3) [n=14]	14.6±1.8 (13.1–17.4) [n=7]	---
HW	7.6±0.6 (6.8–8.4) [n=12]	7±0.5 (6.2–7.9) [n=14]	7.1±1.1 (6.2–8.8) [n=6]	---
HH	7.9±1 (6.5–9.4) [n=12]	6.9±0.6 (5.9–7.8) [n=14]	8±1.4 (6.7–10.3) [n=7]	---
ForeL	19.4±2.1 (15.7–22.4) [n=12]	18.2±0.9 (16.3–20) [n=14]	19.9±1.3 (18.3–21.9) [n=7]	---
HindL	35.9±3.6 (28.8–41.2) [n=12]	33.2±1.6 (30.7–36.3) [n=14]	36.1±4.8 (30.9–44.9) [n=7]	---
Dors	56.1±4.3 (50–67) [n=15]	56.3±4.9 (49–66) [n=19]	55.2±4 (50–62) [n=9]	---
Vent	30.8±1.7 (27–34) [n=25]	31.6±1.3 (28–34) [n=21]	31.2±1.6 (29–34) [n=12]	32 [n=1]
Gul	30.8±2.9 (25–36) [n=20]	29.5±1.9 (25–32) [n=20]	30.1 ±3.1 (25–35) [n=12]	28 [n=1]
Collar	11.5±1 (10–14) [n=20]	11.3±0.9 (10–13) [n=19]	9.3±1.2 (8–11) [n=9]	10 [n=1]
Fpor (L/R)	21.6/20.9±1.4/1.2 (18–24) [n=22/24]	18.5/18.5±2.5/1.9 (14–23) [n=20/22]	22.6/22.6±2.4/1.9 (20–26) [n=12/12]	22/22 [n=1]
Lame	20.2±1.8 (16–23) [n=18]	19.1±1.6 (16–21) [n=21]	18.9±2.4 (16–23) [n=16]	---
Gran	1.2±0.4 (1–2) [n=32]	1.2±0.4 (1–2) [n=29]	1.1±0.15 (1–1.5) [n=21]	1.1±0.2 (1–1.5) [n=7]
Supraoc (L/R)	30.1/30.7±8.7/7.9 (16–48) [n=23/26]	28.4/27.9±7.9/6.7 (18–47) [n=23/25]	19.8/21.1±4/4.5 (13–27) [n=18/15]	22.5/24.7±3.5/3.2 (19–27) [n=4/3]
Temp (L/R)	11.8/11.8±1.4/1.4 (9–15) [n=23/26]	12/11.9±1.2/1.1 (10–14) [n=23/25]	12.1/12.2±1.5/1.6 (9–14) [n=17/16]	12.7/11±2.1/1.4 (10–15) [n=3/2]
Fpor contact	Yes (89%) [n=19]	No (100%) [n=16]	Yes (77%) [n=12]	No (100%) [n=1]
Shape of the upper temporal scales	Pointed [n; males=33; females=26]		Pointed [males, n=22; females, n=4]	
Shape of the lower temporal scales	Smooth [n; males=35; females=27]		Smooth [males, n=26; females, n=6]	
Shape of the dorsal scales	Flat, imbricate and weakly carinate	[n; males=34; females=27]	Pointed/granular and smooth [males, n=17; females, n=3]	
Longitudinal dorsal white stripes/ocelli	Present [n; males=39; females=32]		Fade [n=29]	Present [n=6]
Dorsal black reticulation at midbody	Absent [n; males=36; females=32]		Present [n=29]	Present [n=6]
Number of dorsal stripes	3 [n; males=37; females=32; juveniles=8]		2 [n; males=19; females=6; juveniles=3]	
Colour change from head to tail	Yellowish to white [n; males=18; females=12]		Reddish to yellowish or white/bluish [n=19]	None [n=6]
Ventral tail colour	Blue (Juveniles); Reddish (sub-adult females) [n=8]		Reddish (sub-adults) [n=20]	

TABLE 3. Morphological variables for the holotype and paratypes of *A. margaritae* sp. nov. Variable abbreviations are listed in the Materials and Methods section.

Variable	Holotype		Paratype		Paratype		Paratype	
	MNHN-RA-2016.0105	BEV.9440	MCCI-R.560	MCCI-R.561	MCCI-R.562	Adult, male	Adult, male	Sub-adult, female
SVL	65.1	56	57.9	55.1	42.8			
TailL	130.9	---	96.3	---	77.1			
HL	16.27	12.5	13.8	13.3	11.2			
HW	7.8	6.2	6.8	6.8	5.75			
HH	8.6	7.1	6.65	6.6	5.4			
ForeL	21.2	18.1	16.9	15.7	13.7			
HindL	39.9	33.5	33.2	33.5	26.7			
Dors	55	56	54	55	66			
Vent	33	32	32	31	32			
Gul	33	32	32	34	31			
Collar	11	12	11	12	10			
Fpor (L/R)	21/23	18/17	21/22	22/21	14/14			
Lame	21	20	22	19	16			
Gran	2	1	2	1	1.5			
Supraoc (L/R)	48/44	32/27	47/45	25/26	31/34			
Temp (L/R)	13/13	11/12	13/13	13/12	12/11			
Fpor contact	Yes	No	Yes	Yes	No			
Shape of the upper temporal scales	Pointed	Pointed	Pointed	Pointed	Pointed			
Shape of the lower temporal scales	Smooth	Smooth	Smooth	Smooth	Smooth			
Shape of the dorsal scales	Weakly carinate	Weakly carinate	Weakly carinate	Weakly carinate	Weakly carinate			
Longitudinal dorsal white stripes	Present	Present	Present	Present	Present			
Dorsal black reticulation at midbody	Absent	Absent	Absent	Absent	Absent			

Taxonomic account

The findings from this study support the presence of two separate lineages within *A. busacki*—a northern assemblage from the arid and semi-arid bioclimatic areas between the High Atlas and Anti-Atlas Mountains, and a southern assemblage from the northern Saharan Atlantic coastal desert. These results are evident in both the genetic analyses (Fig. 2; Appendix III) and the morphological comparisons (see above; Tables 2–3; Figs. 4–5). These two lineages are highly divergent genetically (over 12% uncorrected *p*-distance in the *cytb* fragment), to the point that, even if they form a monophyletic clade in the tree (albeit with very low support in both the ML and BI analyses), they are more divergent than all other species within the *pardalis* species-group. Their phenotypical divergence is also stronger than many other species in the *pardalis* species-group (pers. obs.). For all these reasons we prefer to treat these two lineages as two valid species.

Specimen BMNH1970.250 (adult male) was assigned by Salvador (1982) as the holotype of *A. busacki*. This specimen exhibits morphological characters typical of the southern lineage (Figs. 1, 4 & 5). Such features include a very strong black dorsal reticulation with almost undistinguishable longitudinal white lines of ocelli, smooth dorsal scales, and a low number of supraocular granules and collar scales. The nomen *Acanthodactylus busacki* should thus apply to the southern lineage, for which we provide here updated information on distribution, morphology, and ecology. As we did not find any nomen available for the northern lineage, we describe it here as a new species.

Acanthodactylus busacki Salvador, 1982

Acanthodactylus busacki, Salvador, 1982, A revision of the lizards of the genus *Acanthodactylus* (Sauria: Lacertidae), Bonner Zoologische Monographien, Nr. 16: 88.

Chresonyms

Acanthodactylus busacki Salvador, 1982: 88 (part.)

Acanthodactylus pardalis bedriagai Arnold, 1983: 319 (part.)

Acanthodactylus bedriagai Harris & Arnold 2000: 352 (part.)

Acanthodactylus busacki Mellado & Dakki 1988: 175 (part.); Mellado & Olmedo 1990: 133 (part.); Bons & Geniez 1996: 162 (part.); Schleich *et al.* 1996: 391 (part.); Donaire *et al.* 2000: 10; Geniez *et al.* 2004: 102 (part.); Brito *et al.* 2008: 21 (part.); Sindaco & Jeremčenko 2008: 218 (part.); Fonseca *et al.* 2008: 9 (part.); Geniez *et al.* 2010: IUCN red list (part.); Harris *et al.* 2010: 22 (part.); Carretero *et al.* 2011: 139 (part.); Trape *et al.* 2012: 302 (part.); Pyron *et al.* 2013: 17 (part.); Crochet *et al.* 2015: 584; Tamar *et al.* 2016: 8 (part.)

Name-bearing type. Natural History Museum (London) BMNH1970.250, adult male, holotype by original designation.

Type locality. 30 km south-west of Goulimine (= Guelmim), Morocco.

Paratypes. Among the paratypes originally listed by Salvador (1982), MNHN-RA-1938.189 (Asrifa, Morocco), BMNH1970.249 (same locality as the holotype), and EBD2440 (Cape Bojador, Rio de Oro) belong to this species. Other paratypes listed in Salvador (1982) are allocated to the new species (see below) or to *A. cf. maculatus* (Appendix II).

Other material. Ten voucher specimens listed in Appendix II under *A. busacki*, apart from the holotype and paratypes. Photographic material of one voucher specimen from MB and of 25 individuals photographed in the wild is listed in Appendix II.

Diagnosis. A species of the *pardalis* species-group (i.e., small flat or carinated dorsal scales; three series of scales on the fingers; three supraoculars; 12 and sometimes 14 straight longitudinal row of ventrals; slightly pectinate toes; body pattern combining longitudinal rows of light ocelli and black reticulation) characterized by the combination of the following characters: (1) maximum recorded SVL 73 mm (51–73 mm in adult males); (2) three supraoculars, the first supraocular is either entire or fragmented with usually one row of granules between the supraoculars and the superciliaries; (3) 13–27 granules around the supraoculars; (4) subocular with a distinct keel located between the fourth and fifth upper labials and not contacting the lip; (5) upper temporals small and pointed whereas the lower temporals are large and smooth; (6) 8–11 collar scales; (7) 12 longitudinal rows of ventral scales; (8) 29–34 transverse rows of ventral scales; (9) 20–26 femoral pores on each side; (10) three rows of scales on fingers with slight lateral pectination, with 16–23 lamellae underneath the fourth toe; (11) dorsal scales are

pointed and smooth; (12) dorsal colour pattern of juveniles, females and sub-adult males consists of two lateral longitudinal lines of pale ocelli on each side with strong black reticulation among them (four longitudinal dorsal lines in total), adult males have intricate colouration of black reticulation that covers most of the dorsal area and the rows of pale ocelli become indistinct or may completely disappear; (13) the males exhibit a unique colouration: the neck, the posterior part of the throat, the anterior parts of the body and belly, and the forelimbs are more or less reddish; this tint becoming progressively yellowish, whitish or slightly bluish at the posterior parts and tail; (14) sub-adults have reddish or white ventral tail colour.

Distribution. *Acanthodactylus busacki* is found in the northern Saharan Atlantic coastal desert, from around Guelmim in the north to 67 km north-east of Dakhla (Crochet *et al.* 2015) in the south (Fig. 1; Appendix II). Its range is bordered to the north by the southern extension of the Anti-Atlas Mountains. According to Donaire *et al.* (2000) and Geniez *et al.* (2004) the species reaches the Hammada of Tindouf in the extreme south-east of the Atlantic Sahara, entering Algeria and approaching Mauritania, but these records need to be re-examined: they belong to a taxon of the *pardalis* species-group, but not necessarily to *A. busacki*; they might instead involve a desert form of *A. cf. maculatus* entering from the northern Sahara into Algeria and Morocco (J.A. Mateo pers. com.; pers. obs.).

Natural history. *Acanthodactylus busacki* is a ground-dwelling, diurnal, oviparous, medium-sized lizard, relatively large and stout-bodied. It mostly inhabits habitats with hard substratum, most often clay deposits, more rarely rocky ground, always with scattered bushes. It is widely sympatric with *A. aureus* which occurs on sandy substratum (pers. obs.; Geniez *et al.* 2004). Reddish ventral tail colouration of sub-adults is present in all populations of this species, and not only in the southern populations (*contra* Crochet *et al.* 2015).

***Acanthodactylus margaritae* sp. nov.**

(Tables 1–3; Figs. 1–8; Appendices I–III)

Chresonyms

Acanthodactylus busacki Salvador, 1982: 88 (part.)

Acanthodactylus pardalis bedriagai Arnold, 1983: 319 (part.)

Acanthodactylus bedriagai Harris & Arnold 2000: 352 (part.)

Acanthodactylus busacki Mellado & Dakki 1988: 175 (part.); Mellado & Olmedo 1990: 133 (part.); Bons & Geniez 1996: 162 (part.); Schleich *et al.* 1996: 391 (part.); Geniez *et al.* 2004: 102 (part.); Brito *et al.* 2008: 21 (part.); Sindaco & Jeremčenko 2008: 218 (part.); Fonseca *et al.* 2008: 9 (part.); Harris *et al.* 2010: 22 (part.); Barata *et al.* 2011: 7 (part.); Carretero *et al.* 2011: 139 (part.); Trape *et al.* 2012: 302 (part.); Pyron *et al.* 2013: 17 (part.); Tamar *et al.* 2016: 8 (part.)

Name bearing type. Muséum national d'Histoire naturelle (Paris) MNHN-RA-2016.0105 (formerly BEV.9439, tissue sample in the BEV tissue collection, code T1176), adult male, collected on the 11th of February 2008 by P.-A. Crochet (Fig. 6).

Type locality. 500 m north-east of Sidi Binzarne, approximately 3 km south-east of Sidi R'bat (Massa), Morocco, 30.0580°N, 9.6456°W (WGS84).

Paratypes. BEV.9440 (tissue sample code T1177, adult female, collected in the Ademine forest 1.6 km past the Agadir-Taroudant road towards Biougra, Morocco, 30.31579°N 9.36004°W, on the 11th of February 2008 by P.-A. Crochet); MCCI-R.560 (adult male, collected from between Inchaden and Tifnite, Morocco, 30.15°N, 9.59°W, on the 9th of May 1993 by R. Sindaco and N. Fedrighini); MCCI-R.561 (adult male, collected from Souss valley, outskirts of Biougra, Morocco, 30.21°N, 9.38°W, on the 9th of May 1993 by R. Sindaco and N. Fedrighini); MCCI-R.562 (sub-adult female, collected from Souss valley, outskirts of Biougra, Morocco, 30.21°N 9.38°W, on the 9th of May 1993 by R. Sindaco and N. Fedrighini) (Fig. 7).

Other material. Thirty-three voucher specimens listed in Appendix II under *A. margaritae* sp. nov. apart from the holotype and paratypes. Photographic material of 19 voucher specimens from the BMNH, CAS, FMNH, MB, and ZMH are listed in Appendix II, and of 29 individuals photographed in the wild (only meristic characters and colouration documented; Appendix II).

Etymology. The specific epithet “*margaritae*”, a noun in the genitive case, honours Dr Margarita Metallinou who tragically lost her life during field-work in Africa in July 2015. The new species is dedicated to Margarita Metallinou from all the authors in recognition of her passion, interest and strong contribution to the study of reptile

systematics (especially of geckoes of the genera *Stenodactylus* and *Ptyodactylus*) and to her friendship over the years.

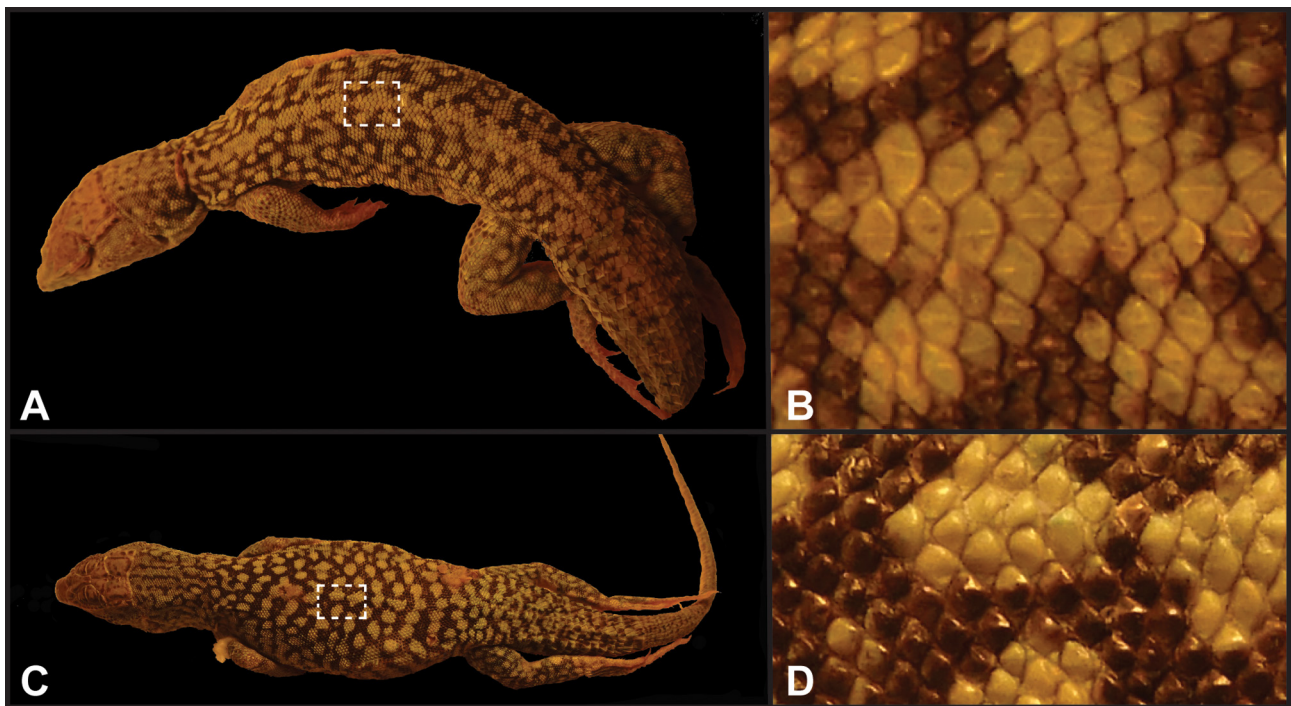


FIGURE 4. Comparison of dorsal scales of adult males. A–B) *Acanthodactylus margaritae* sp. nov. (BEV.5504); C–D) *A. busacki* (BEV.11435). Photos by Karin Tamar.

Diagnosis. A new species of the *pardalis* species-group (i.e., small flat or carinated dorsal scales; three series of scales on the fingers; three supraoculars; 12 and sometimes 14 straight longitudinal row of ventrals; slightly pectinate toes; body pattern combining longitudinal rows of light ocelli and black reticulation) from between the High Atlas and Anti-Atlas Mountains characterized by the combination of the following characters: (1) maximum recorded snout-vent length 71 mm (54–71 mm in adult males and 54–64.7 mm in adult females); (2) three supraoculars, the first supraocular is either entire or fragmented with usually one row of granules between the supraoculars and the superciliaries; (3) 16–48 granules around the supraoculars (mean 29.7); (4) subocular with a distinct keel is situated between the fourth and fifth upper labials and does not contact the lip; (5) upper temporals small and pointed whereas the lower temporals are large and smooth; (6) 10–14 collar scales; (7) usually 12 longitudinal rows of ventral scales; (8) 27–34 (mean 31.2) ventral transverse rows; (9) 14–24 (mean 21.1) femoral pores on each side (higher number in males; 14–23 in females vs. 18–24 in males; mostly in contact in males, separated in females); (10) three rows of scales on fingers with slight lateral pectination, with 16–23 (mean 19.5) lamellae underneath the fourth toe; (11) dorsal scales weakly carinated, flat and imbricate; (12) dorsal colour pattern consists of three longitudinal pale lines or rows of whitish, elongated ocelli on each side (six longitudinal dorsal lines in total), with obvious black reticulation between the two outer ones and no or little reticulation between the inner ones on the middle of the dorsum; (13) the dorsal and ventral scales of the nape and body show yellowish colouration in both males and females during the spring, which fades later during the summer; (14) juveniles have blue colouration of the tail, and sub-adult females sometimes have a reddish ventral tail colour.

Differential diagnosis. *Acanthodactylus margaritae* sp. nov. is a typical member of the *pardalis* species-group, differing from the other geographically-close members of the species-group by the following characters:

Acanthodactylus margaritae sp. nov. differs from *A. busacki* in having weakly carinated, irregular and imbricate dorsal scales (vs. small, pointed or granular, and smooth in *A. busacki*; Fig. 4).

Acanthodactylus margaritae sp. nov. further differs from *A. busacki* in its colour pattern (Figs. 4–8): it has three pale longitudinal lines or series of ocelli on each side of the body, six lines in total (vs. two on each side, four in total in *A. busacki*). It also exhibits a moderate sexual dimorphism (stronger in *A. busacki*) and less marked ontogenic changes (Figs. 5–8). Juveniles, females and males of *A. margaritae* sp. nov. all present the typical

pattern of three whitish stripes or series of ocelli on each side (six in total). Juvenile, females and sub-adult males of *A. busacki* have two whitish stripes or series of ocelli on each side but these pale lines disappear or become indistinct in many adult males of *A. busacki* (they remain obvious in adult males of *A. margaritae* **sp. nov.**).

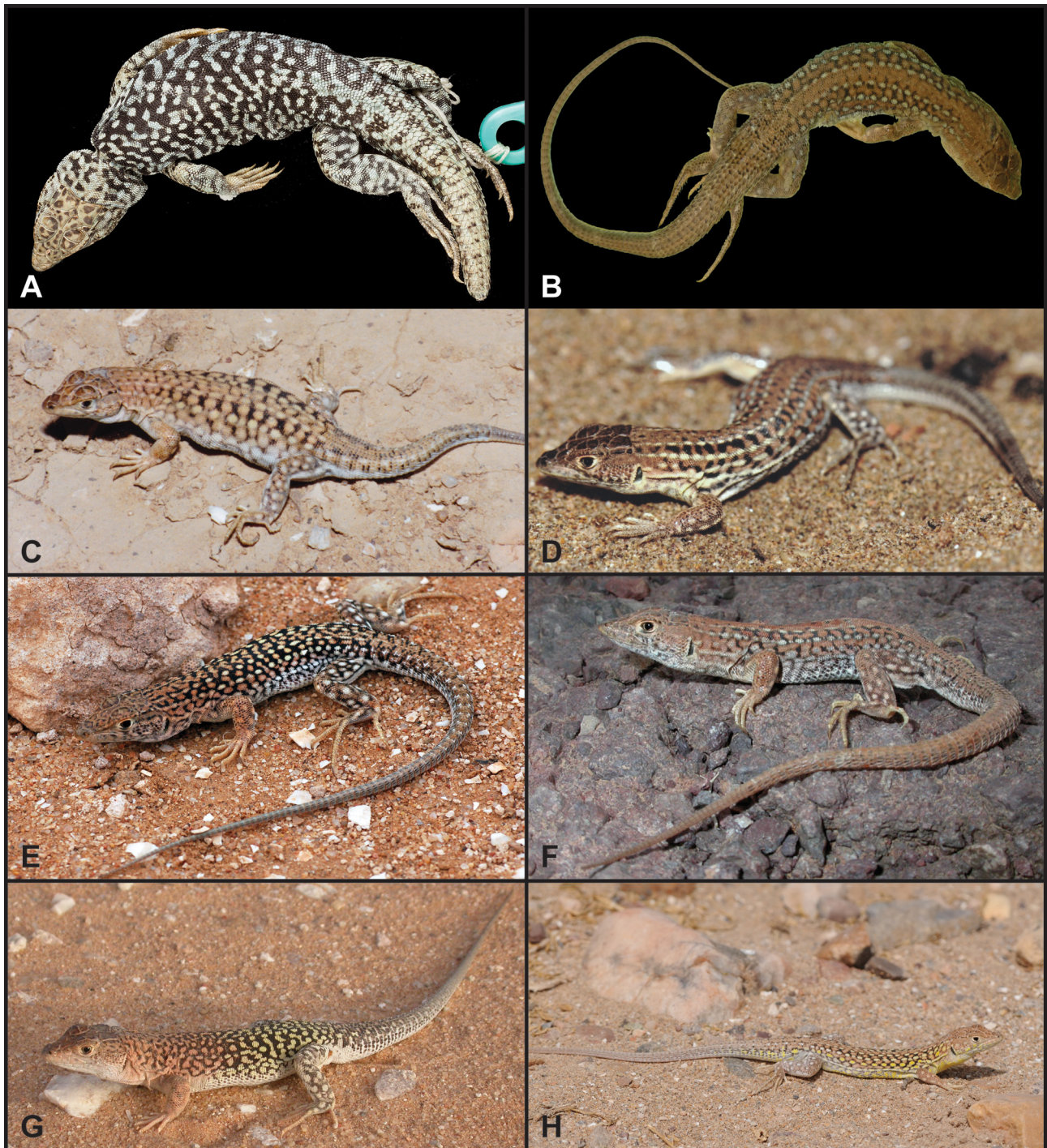


FIGURE 5. Comparison of dorsal colour patterns. A) *Acanthodactylus busacki*, holotype, adult male (BMNH1970.250), photo by Patrick Campbell; B) *A. margaritae* **sp. nov.**, holotype, adult male (MNHN-RA-2016.0105), photo by Pierre-André Crochet; C) *A. busacki*, adult female (PGe.154), photo by Michel Geniez; D) *A. margaritae* **sp. nov.**, adult female (PGe.1143), photo by Alexandre Cluchier; E) *A. busacki*, adult male (PGe.1167), photo by Gabriel Martínez & Raúl León; F) *A. margaritae* **sp. nov.**, adult male (PGe.1170), photo by Barny Barnestein; G) *A. busacki*, adult male (BEV.10829), photo by Pierre-André Crochet; H) *A. margaritae* **sp. nov.**, adult male (PGe.1176), photo by Jean-Michel Bompar.

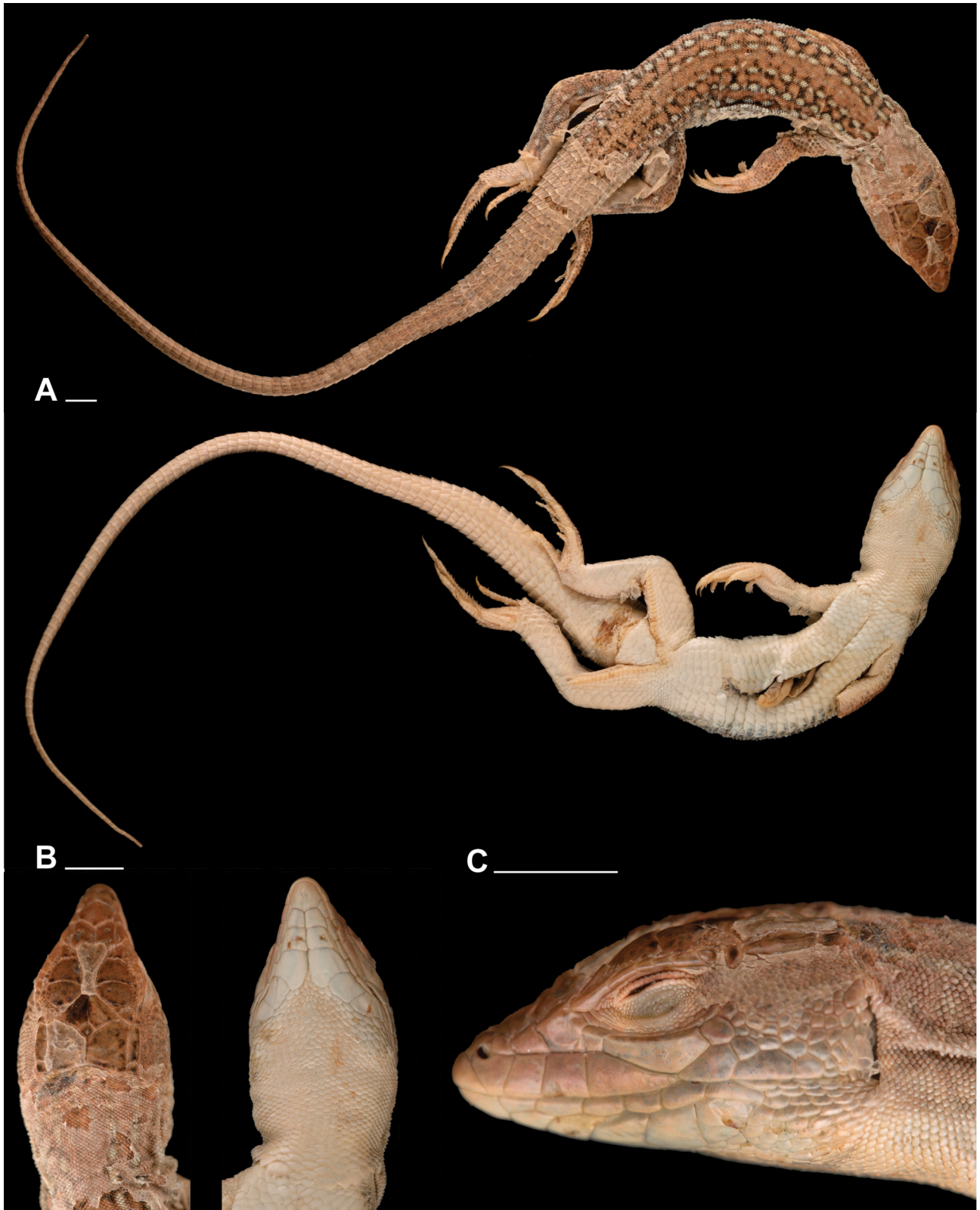


FIGURE 6. Holotype of *Acanthodactylus margaritae* **sp. nov.** MNHN-RA-2016.0105 (former BEV.9439), adult male. A) Habitus, dorsal and ventral views; B) Head, dorsal and ventral views; C) Lateral head view. Scale bars = 5 mm. Photos by Oz Rittner.

The colour pattern of adult males of the two species is thus usually quite different. Adult males of *A. margaritae* **sp. nov.** still exhibit three whitish stripes or series of ocelli on each side of the body with weak or no dark reticulation between the inner ones on the middle of the dorsum. In adult males of *A. busacki* the two whitish

stripes or series of ocelli tend to disappear into a pattern of strong dark reticulation that extends to the middle of the back between the two inner pale stripes. Adult males of *A. margaritae* **sp. nov.** have a yellowish colour over the anterior dorsal and ventral areas, in *A. busacki* males acquire a reddish/pink colouration on the neck and upper dorsum contrasting with yellowish colouration at the lower dorsum and white ventral areas.

Adult females of the two species differ in the number of pale longitudinal lines (see above), in the absence (in *A. margaritae* **sp. nov.**) or presence (*A. busacki*) of dark reticulation on the middle of the dorsum, and in the presence (in *A. margaritae* **sp. nov.**) or absence (in *A. busacki*) of yellowish colouration on the anterior part of the body (see also Table 2).

Less marked and non-diagnostic differences in males also include a higher number of collar scales (10–14 in *A. margaritae* **sp. nov.** vs. 8–11 in *A. busacki*; $P < 0.0001$), a higher number of granules around the supraoculars (16–48 in *A. margaritae* **sp. nov.** vs. 13–27 in *A. busacki*; $P < 0.0001$), and a lower number of femoral pores on the right side (18–24 in *A. margaritae* **sp. nov.** vs. 20–26 in *A. busacki*; $P = 0.017$) (Table 2).

Acanthodactylus margaritae **sp. nov.** differs from the north-eastern Moroccan populations classified as *A. maculatus* by Bons and Geniez (1996, probably a composite assemblage of several species; Fig. 2) in having weakly keeled dorsal scales (vs. flat dorsal scales in *A. cf. maculatus*). It further differs in having small and pointed upper temporals and large and smooth lower temporals (vs. granular and flat upper temporals that gradually increase in size in *A. cf. maculatus*); by having 10–14 collar scales (vs. 8–11 in *A. cf. maculatus*); a higher number of granules around the supraoculars (16–48 vs. 14–21, respectively); and by the absence of a small upper labial scale beneath the subocular (at time present in *A. cf. maculatus*). In addition, *A. margaritae* **sp. nov.** is slenderer than *A. cf. maculatus* which is more robust and stubby with a shorter tail, especially females.

Description of the holotype. Habitus robust (Fig. 6). Total length 196 mm (SVL 65.1 mm; un-regenerated tail 130.9 mm). The head presents a well-defined lanceolate concavity from the frontal to the supranasal scales. Snout is pointed, but not very narrow. Rostral shield is not prominent, followed by paired supranasals, their suture very short. Frotonasal is hexagonal and slightly broader than long. Prefrontals are longer than broad; the length of the suture is almost as long as their width. Frontal is narrow and long, broader anteriorly than posteriorly; its length is almost its distance from the tip of the snout. Frontoparietals suture is almost half the length of the frontal, and almost the same length at their posterior margins with the parietals. Parietals are rather broader than longer. Interparietal is relatively large with a diamond shape and a clear parietal foramen; its length equals to its width. Occipital scale is absent. Three supraoculars, the first supraocular is broken into two fragments, the second and third supraoculars intact; six supraciliaries on each side, the first is the longest; 48/44 (left/right) supraciliary granules arranged in two continuous rows contacting the inner border of supraciliaries on each side. Nostrils situated at the cross-point of three scales, bordered dorsally by the supranasal, posteriorly by a single postnasal, and inferiorly by the first upper labial, which is broader above than below. Two loreal scales, the anterior one smaller, the posterior longer and in contact with the anterior first supraciliaries and subocular. Two suboculars with a sharp keel close to their upper margin, the anterior smaller, the posterior longer and wedged between the fourth and fifth upper labials, not contacting the lip. Scales along the upper margin of the suboculars are long and thin, followed by the postocular scales. Upper postocular in contact with the anterior supratemporal, separated from the posterior supraciliary and the supraoculars by granules. Scales in centre of lower eyelid small, round and granular. Seven upper labials on each side, four anterior to the subocular; the fourth upper labial is the longest, followed by the fifth. Two keeled supratemporals, the anterior longer than the posterior. Upper temporals small, pointed and granular, progressively larger and smoother towards the upper labials. A small tympanic scale is present. Anterior margin of the ear opening with six denticulations on each side, the middle four larger and subtriangular. Six lower labials on either side. Five pairs of submaxillaries, the three anterior from each side in contact in the middle. There are 33 gular scales in a straight line between the symphysis of the submaxillaries and the median collar plate, slightly enlarged and imbricate towards the collar; gular fold absent. Collar curved, composed of 11 scales.

Dorsal scales are small and pointed at the nape, slightly larger and weakly keeled between the limbs, becoming larger and flat with a keel on the tail; 55 rows of dorsal scales at midbody. Scales on the flanks are small, almost granular, pointed or slightly keeled, becoming larger and flat ventrally. Ventral scales arranged in 12 longitudinal rows and 33 transverse rows, arranged anteriorly in oblique transverse rows. Three enlarged preanal plates in a transversal row between the anterior cloacal margin and the gap between the two series of femoral pores. Two continuous rows of 21/23 femoral pores, the two series are in contact anteriorly and extending close to the knee.

Dorsal surfaces of the limbs covered by medium sized, imbricate, keeled scales; anterior surface of the limbs

covered by larger, unkeeled, imbricate scales; posterior covered with smaller granular scales. The right forelimb is amputated just before the fingers. The ventral side of the forelimbs is covered with small, smooth scales; ventral surface of hind limbs covered with large flat scales. Three longitudinal rows of scales on the toes, except the first which has only two; pectination along the toes is weak; 21 smooth sub-digital lamellae under the fourth toe.

Upper caudal scales are rectangular, larger than the posterior dorsals, flat and keeled; small scales are situated in a longitudinal straight line at the base of the tail on the vertebral row; ventral scales large and smooth.



FIGURE 7. Four paratypes of *Acanthodactylus margaritae* sp. nov. A–B) BEV.9440, adult female; C–D) MCCI-R.560, adult male; E–F) MCCI-R.561, adult male; G–H) MCCI-R.562, sub-adult female. Scale bars = 5 mm. Photos by Oz Rittner and Pierre-André Crochet.

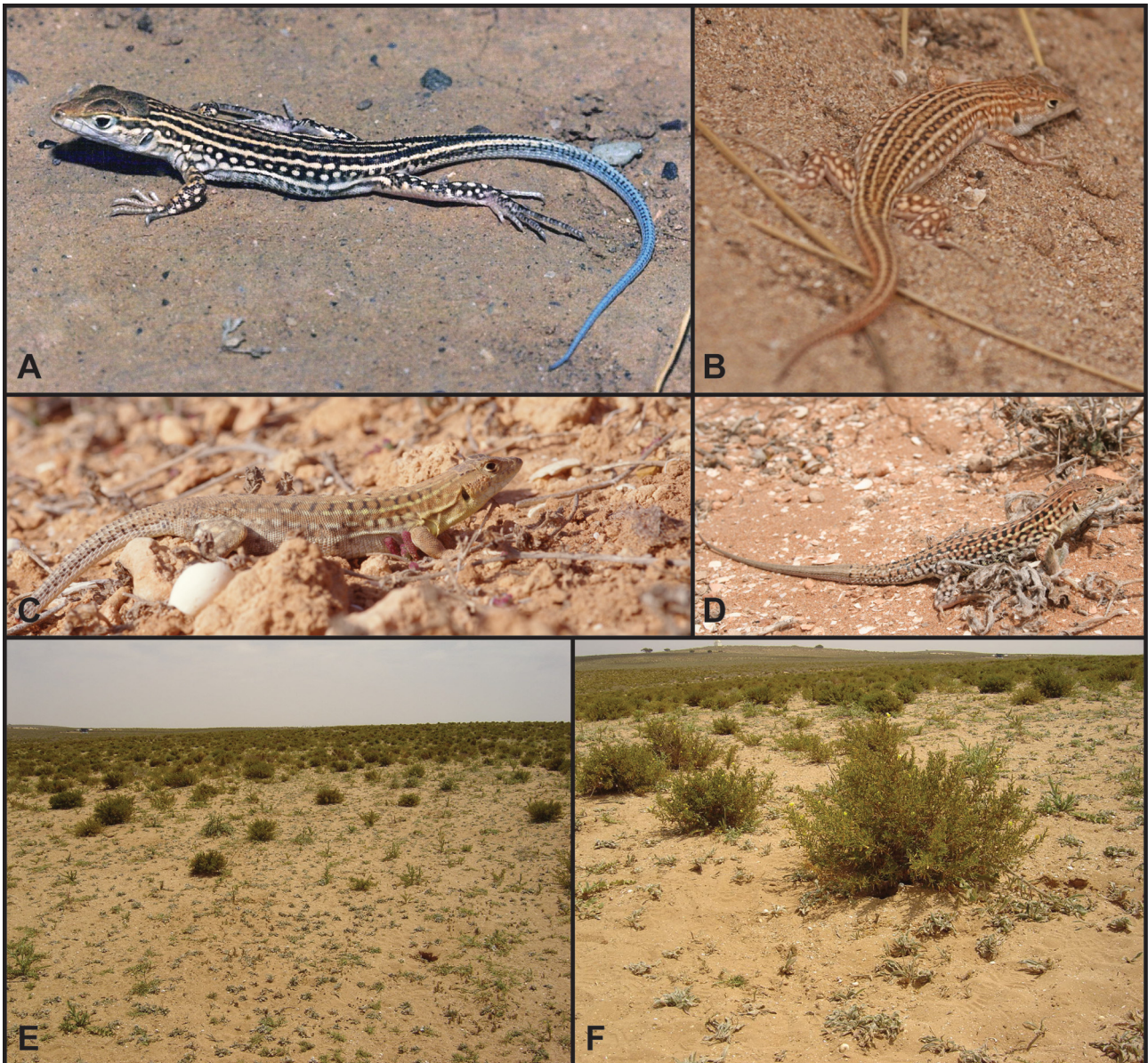


FIGURE 8. Live specimens of *Acanthodactylus margaritae* sp. nov. and natural habitats. A) juvenile (PGe.150), photo by Philippe Geniez; B) sub-adult female (PGe.1147), photo by Sébastien Durand; C) adult female (PGe.1174), photo by Hugo Cayuela; D) adult male (PGe.1173), photo by Raul León; E–F) Oued Massa, Agadir-Tiznit, Morocco, photos by José C. Brito.

Background colouration in alcohol mainly brown. Pileus brown, head becoming brighter-whitish from the upper and lower labials ventrally, white inframaxillars. Dorsum brown with three lines of white ocelli extending from the nape to the tail; the central lines close to the centre of the dorsum start from the mid parietals and extend to the base of the tail. The middle lines start from the posterior supratemporals and continue to the sides of the tail. The outer lines are made of roundish ocelli and extend from the temporals to the hind-limbs. A black reticulation is present between the outer and middle lines, but is much reduced between the two inner lines. Fore and hind limbs with dark reticulation and white spots on a brown background. The entire underside of the head, body, limbs and tail is white.

Variation. The paratypes do not differ substantially from the holotype in the meristic or discrete characters, varying slightly in size related measurements (Table 3). Paratype MCCI-R.560 has a partially broken tail at a third of its length, and paratypes MCCI-R.561 and BEV.9440 both have broken tails, but, in the former, the severed tail is preserved intact together with the specimens (Fig. 7). The number of femoral pores is lower in the two female paratypes, MCCI-R.562 and BEV.9440, for which the femoral rows are also not in contact.

Colour and pattern of the adults of both sexes are similar to that of the holotype (based on the photographic

material of individuals in the wild). Head dorsally brown with dark brown or black spots. Laterally the upper and lower labials are brighter with dark spots, and the gulars are whitish. The dorsum has a grey/brown background with three longitudinal whitish stripes (in juveniles) or series of ocelli (sub-adults and adults) on each side, starting from the back of the head. An additional whitish stripe is at the border between the dorsals and ventrals. A black reticulation is present among the stripes, which fades closer to the head, or present at lesser amount at midbody between the two central stripes. Adult males and females (prominent in males, not seen in alcohol) exhibit lateral yellow colouration from head to tail on the dorsum and ventrals during the spring; this yellowish colouration fades during the summer. Between the three dorsal stripes on each side, the two central stripes meet at the base of the tail, whereas the two lateral stripes continue along the tail (more obvious in juveniles). The tail is dorsally brown with transverse, continuous or discontinuous black bands laterally and between the two whitish stripes. The limbs have an irregular black and brownish background with whitish spots; this pattern is less obvious on the forelimbs. The ventral colour is off-white. Juveniles exhibit a more prominent contrast of colours on the dorsum and limbs. Juveniles have a blackish ground colour with four shining creamy longitudinal stripes on the dorsum and a row of ocelli of the same colour on each flank; the two median dorsal light stripes come together at the base of the tail while the blackish ground colour continues until the first third part of the tail; the tail is bluish to shining blue (Fig. 8).

Distribution. *Acanthodactylus margaritae* **sp. nov.** is endemic to Morocco (Fig. 1), from around 10 km north of Tamri in the north to Tiznit surroundings in the south (southernmost known locality: 3 km north-east of Sidi Boulfadail; PGe.151 & 152), and along the Souss valley to the east, as far as 25 km east of Taroudant (present study; PGe.150), but probably as far as Aoulouz (Salvador 1982; Bons & Geniez 1996). Its range is limited by the High Atlas and Anti-Atlas Mountains to the north, east and south, and is entirely included in the arid and semi-arid climates with warm or temperate winters (Bons & Geniez 1996).

Natural history. *Acanthodactylus margaritae* **sp. nov.** is a ground-dwelling, diurnal, oviparous, medium-sized lizard, relatively large and stout-bodied. It mostly inhabits stony plains with fine grained soils, stable sands and fixed dunes, or hard clay grounds with scarce low vegetation but also, especially in the Souss valley, open argan tree forests. It is often sympatric with *Acanthodactylus aureus* in the coastal area, though the latter species prefers softer, looser sands.

Discussion

Our study, as well as the previous phylogenetic works of Fonseca *et al.* (2008) and Tamar *et al.* (2016), have showed that what has been considered as *Acanthodactylus busacki* until now in fact comprises two distinct species – the southern *A. busacki* and the northern *A. margaritae* **sp. nov.**, with a level of genetic divergence typical of other closely-related species within the genus *Acanthodactylus* (Tamar *et al.* 2016).

The south-western part of the Anti-Atlas Mountains separates the known distribution of the two species and no specimens are currently known from the area separating them (70 km without known records of the *pardalis* species-group between the distribution areas of *A. margaritae* **sp. nov.** and *A. busacki*). They are thus probably allopatric, although further work in the sandy coastal habitats at the western edge of the Anti-Atlas Mountains (Sidi Ifni area) might reveal additional populations in the current distribution gap. The High Atlas Mountains seem to separate *A. margaritae* **sp. nov.** from the fringe-fingered lizards of the *erythrurus* species-group.

The Atlas Mountains are a series of mountain ranges that extend for around 2500 km in a southwest-northeast direction from Morocco into Algeria and Tunisia, with several peaks of more than 4000 m elevation. The Moroccan Atlas Mountains were formed by the reactivation of a major intracontinental rift system during the African and European plates' convergence in the Neogene and Quaternary (Dewey *et al.* 1989). The main episode of uplifting began around the middle to late Miocene ca. 5–15 million years ago (Mya; Gomez *et al.* 2000). The alluvial basin of the Souss valley is bordered to the north by the High Atlas Mountains, to the south by the Anti-Atlas and to the east by the volcanic massif of Jebel Sirwa (Fig. 1; Bhiry & Occhietti 2004). The narrow eastern part of the Souss valley is characterized by hard ground and coarse deposits, while the wide western coastal area consists mainly of fluvial terraces with aeolian dunes along the coastline and inland (Bhiry & Occhietti 2004). The south-western extension of the Anti-Atlas Mountains may, according to the geographic distributions, represent the biogeographical barrier between *A. margaritae* **sp. nov.** and *A. busacki*, limiting the former to the Souss valley and

adjacent areas in Morocco. The divergence time estimates for *Acanthodactylus*, published in Tamar *et al.* (2016), suggests that the speciation time between *A. busacki* (southern clade) and *A. margaritae* **sp. nov.** (northern clade) took place during the late Pliocene, ca. 4.7 million years ago (95% highest posterior density 2.8–7.1 Mya). This date corresponds to the final uplifting process of the Anti-Atlas range as the land masses of Europe and Africa collided. That said, given the dynamic environment during the late Neogene (see Fonseca *et al.* 2008, 2009; Tamar *et al.* 2016 for more details) and with the data at hand, other factors such as the changing climate and soils may also be the cause enabling speciation between these two *Acanthodactylus* species.

Acanthodactylus busacki, including *A. margaritae* **sp. nov.** within its distribution range, is currently listed in the IUCN Red List of Threatened Species as Least Concern (Geniez *et al.* 2010). The local and global conservation status of *A. margaritae* **sp. nov.** and that of *A. busacki* should be re-evaluated based on the present taxonomic revision and the probable endemism of *A. margaritae* **sp. nov.** and its limited distribution in Morocco. The taxonomic change presented in this study calls for the separation of the two species and for a re-evaluation of conservation measures, especially since the natural habitats in the Souss valley have been under considerable pressure from agriculture and other human impacts in the last few decades.

Acknowledgements

We wish to thank the following people for their help with the provision of samples and shipment or photographs of specimens: Roberto Sindaco (MCCI; Museo Civico di Storia Naturale, Carmagnola, Turin, Italy), Luis M.P. Ceriaco (MUHNAC; Museu Nacional de História Natural e da Ciência, Lisbon, Portugal), Wolfgang Böhme, Dennis Rödder and Ursula Bott (ZFMK; Zoologisches Forschungsmuseum Alexander Koenig, Bonn, Germany), Jens Vindum and Noel Graham (CAS; California Academy of Sciences, San Francisco, USA), Alan Resetar (FMNH; Field Museum of Natural History, Chicago, USA), Patrick Campbell (BMNH; Natural History Museum, London, England), and Annemarie Ohler, Laure Pierre and Nicolas Vidal (MNHN; Muséum national d'Histoire naturelle, Paris, France). We are grateful to the following people for providing photographic material: Barny Barnestein, Patrick Bergier, Jean-Michel Bompar, Luís García Cardenete, Hugo Cayuela, Alexandre Cluchier / ECO-MED, David Donaire, Sébastien Durand, Michel Geniez, Raúl León, Gabriel Martínez, Juan-Manuel Pleguezuelos, and Xavier Rufay. We are especially grateful to Oz Rittner for his help with the photographs of the holotype and paratypes. J.C.B. is supported by Fundação para a Ciência e Tecnologia (IF/459/2013). K.T. was supported by the Steinhardt Museum of Natural History, Israel National Centre for Biodiversity Studies, Tel Aviv University, Israel.

References

- Arnold, E.N. (1983) Osteology, genitalia and the relationships of *Acanthodactylus* (Reptilia: Lacertidae). *Bulletin of the British Museum (Natural History)*, Zoology, 44, 291–339.
- Bandelt, H.J., Forster, P. & Röhl, A. (1999) Median-joining networks for inferring intraspecific phylogenies. *Molecular Biology and Evolution*, 16, 37–48.
<https://doi.org/10.1093/oxfordjournals.molbev.a026036>
- Barata, M., Perera, A., Harris, D.J., Van der Meijden, A., Carranza, S., Ceacero, F., García-Muñoz, E., Gonçalves, D., Henriques, S., Jorge, F. & Marshall, J.C. (2011) New observations of amphibians and reptiles in Morocco, with a special emphasis on the eastern region. *British Herpetological Society Herpetological Bulletin*, 116, 4–14.
- Bhiry, N. & Occhietti, S. (2004) Fluvial sedimentation in a semi-arid region: the fan and interfan system of the Middle Souss Valley, Morocco. *Proceedings of the Geologists' Association*, 115, 313–324.
[https://doi.org/10.1016/S0016-7878\(04\)80011-7](https://doi.org/10.1016/S0016-7878(04)80011-7)
- Bons, J. & Geniez, P. (1996) *Amphibiens et reptiles du Maroc*. Asociación Herpetológica Española, Barcelona, 319 pp.
- Brito, J.C., Rebelo, H., Crochet, P.-A. & Geniez, P. (2008) Data on the distribution of amphibians and reptiles from North and West Africa, with emphasis on *Acanthodactylus* lizards and the Sahara Desert. *Herpetological Bulletin*, 105, 19–27.
- Carretero, M.A., Fonseca, M.M., Garcia-Munoz, E., Brito, J.C. & Harris, D.J. (2011) Adding *Acanthodactylus beershebensis* to the mtDNA phylogeny of the *Acanthodactylus pardalis* group. *North-Western Journal of Zoology*, 7, 138–142.
- Castresana, J. (2000) Selection of conserved blocks from multiple alignments for their use in phylogenetic analysis. *Molecular Phylogenetics and Evolution*, 17, 540–552.
<https://doi.org/10.1093/oxfordjournals.molbev.a026334>

- Crochet, P.-A., Geniez, P. & Ineich, I. (2003) A multivariate analysis of the fringe-toed lizards of the *Acanthodactylus scutellatus* group (Squamata: Lacertidae): systematic and biogeographical implications. *Zoological Journal of the Linnean Society*, 137, 117–155.
<https://doi.org/10.1046/j.1096-3642.2003.00044.x>
- Crochet, P.-A., Leblois, R. & Renoult, J.P. (2015) New reptile records from Morocco and Western Sahara. *Herpetology Notes*, 8, 583–588.
- Dewey, J.F., Helman, M.L., Turco, E., Knott, S.D. & Hutton, D.H.W. (1989) Kinematics of the western Mediterranean. *Geological Society, London, Special Publications*, 45, 265–283.
<https://doi.org/10.1144/GSL.SP.1989.045.01.15>
- Donaire, D., Mateo, J.A., Hasi, M. & Geniez, P. (2000) Nuevos datos sobre la fauna reptiliana de la Hamada de Tinduf (Argelia). *Boletín de la Asociación Herpetológica Española*, 11, 8–12.
- Drummond, A.J., Suchard, M.A., Xie, D. & Rambaut, A. (2012) Bayesian phylogenetics with BEAUti and the BEAST 1.7. *Molecular Biology and Evolution*, 29, 1969–1973.
<https://doi.org/10.1093/molbev/mss075>
- Fitzinger L.J.F.J. (1834). *Acanthodactylus*. In: Wiegman A.F.A. (Ed.), *Herpetologia mexicana, seu Descriptio amphibiorum Novae Hispaniae quae itineribus comitis De Sack, Ferdinandi Deppe et Chr. Guil. Schiede in Museum zoologicum Berolinense pervenerunt. Pars prima saurorum species amplectens, adjecto systematis saurorum prodromo, additisque multis in hunc amphibiorum ordinem observationibus*. C. G. Luderitz, Berolini, pp. 10.
- Flot, J.F. (2010) SeqPHASE: a web tool for interconverting PHASE input/output files and FASTA sequence alignments. *Molecular Ecology Resources*, 10.1, 162–166.
<https://doi.org/10.1111/j.1755-0998.2009.02732.x>
- Fonseca, M.M., Brito, J.C., Paulo, O.S., Carretero, M.A. & Harris, D.J. (2009) Systematic and phylogeographical assessment of the *Acanthodactylus erythrurus* group (Reptilia: Lacertidae) based on phylogenetic analyses of mitochondrial and nuclear DNA. *Molecular Phylogenetics and Evolution*, 51, 131–142.
<https://doi.org/10.1016/j.ympev.2008.11.021>
- Fonseca, M.M., Brito, J.C., Rebelo, H., Kalboussi, M., Larbes, S., Carretero, M.A. & Harris, D.J. (2008) Genetic variation among spiny-footed lizards in the *Acanthodactylus pardalis* group from North Africa. *African Zoology*, 43, 8–15.
<https://doi.org/10.1080/15627020.2008.11407401>
- Geniez, P., Mateo, J.A., Geniez, M. & Pether, J. (2004) *The amphibians and reptiles of the Western Sahara (former Spanish Sahara) and adjacent regions*. Edition Chimaira, Frankfurt, 228 pp.
- Geniez, P., Mateo Miras, J.A., Joger, U., Pleguezuelos, J., Slimani, T. & El Mouden, E.H. (2010) *Acanthodactylus busacki*. The IUCN Red List of Threatened Species 2010: e.T178569A7572735. Available from: <http://www.iucnredlist.org/details/178569/0> (accessed 24 April 2017)
- Gomez, F., Beauchamp, W. & Barazangi, M. (2000) Role of the Atlas Mountains (northwest Africa) within the African-Eurasian plate-boundary zone. *Geology*, 28, 775–778.
[http://dx.doi.org/10.1130/0091-7613\(2000\)28<775:ROTAMN>2.0.CO;2](http://dx.doi.org/10.1130/0091-7613(2000)28<775:ROTAMN>2.0.CO;2)
- Harris, D.J. & Arnold, E.N. (2000) Elucidation of the relationships of spiny footed lizards, *Acanthodactylus* spp. (Reptilia: Lacertidae) using mitochondrial DNA sequence, with comments on their biogeography and evolution. *Journal of Zoology*, 252, 351–362.
<https://doi.org/10.1111/j.1469-7998.2000.tb00630.x>
- Harris, D.J., Batista, V. & Carretero, M. (2004) Assessment of genetic diversity within *Acanthodactylus erythrurus* (Reptilia: Lacertidae) in Morocco and the Iberian Peninsula using mitochondrial DNA sequence data. *Amphibia-Reptilia*, 25, 227–232.
<https://doi.org/10.1163/1568538041231229>
- Harris, D.J., Perera, A., Barata, M., Tarroso, P. & Salvi, D. (2010) New distribution notes for terrestrial herpetofauna from Morocco. *North-Western Journal of Zoology*, 6, 309–315.
- Huelsenbeck, J.P. & Rannala, B. (2004) Frequentist properties of Bayesian posterior probabilities of phylogenetic trees under simple and complex substitution models. *Systematic Biology*, 53.6, 904–913.
<https://doi.org/10.1080/10635150490522629>
- Katoh, K. & Standley, D.M. (2013) MAFFT multiple sequence alignment software version 7: improvements in performance and usability. *Molecular Biology and Evolution*, 30, 772–780.
<https://doi.org/10.1093/molbev/mst010>
- Kumar, S., Stecher, G. & Tamura, K. (2016) MEGA7: Molecular Evolutionary Genetics Analysis version 7.0 for bigger datasets. *Molecular Biology and Evolution*, 33, 1870–1874.
<https://doi.org/10.1093/molbev/msw054>
- Lanfear, R., Frandsen, P.B., Wright, A.M., Senfeld, T. & Calcott, B. (2016) PartitionFinder 2: new methods for selecting partitioned models of evolution for molecular and morphological phylogenetic analyses. *Molecular Biology and Evolution*, 34, 772–773.
<https://doi.org/10.1093/molbev/msw260>
- Librado, P. & Rozas, J. (2009) DnaSP v5: A software for comprehensive analysis of DNA polymorphism data. *Bioinformatics*, 25, 1451–1452.

- <https://doi.org/10.1093/bioinformatics/btp187>
- Mellado, J. & Dakki, M. (1988) Inventaire commenté des amphibiens et reptiles du Maroc. *Bulletin de l'Institut Scientifique, Rabat*, 12, 171–181.
- Mellado, J. & Olmedo, G. (1990) El género *Acanthodactylus* en Marruecos: problemas de identificación en los grupos de especies *A. pardalis* y *A. scutellatus*. *Amphibia-Reptilia*, 11, 131–146.
<https://doi.org/10.1163/156853890X00537>
- Pyron, R.A., Burbrink, F.T. & Wiens, J.J. (2013) A phylogeny and revised classification of Squamata, including 4161 species of lizards and snakes. *BMC Evolutionary Biology*, 13, 93.
<https://doi.org/10.1186/1471-2148-13-93>
- Rambaut, A., Suchard, M.A., Xie, D. & Drummond, A.J. (2014) Tracer v1.6. Available from: <http://beast.bio.ed.ac.uk/Tracer> (accessed 24 April 2017)
- Salvador, A. (1982) A revision of the lizards of the genus *Acanthodactylus* (Sauria: Lacertidae). *Bonner Zoologisches Monographien*, Nr. 16, Zoologisches Forschungsinstitut und Museum Alexander Koenig, 1–167.
- Schleich, H.H., Kästle, W. & Kabisch, K. (1996) *Amphibians and reptiles of North Africa*. Koeltz, Koenigstein, 627 pp.
- Silvestro, D. & Michalak, I. (2012) raxmlGUI: a graphical front-end for RAXML. *Organisms Diversity & Evolution*, 12.4, 335–337.
<https://doi.org/10.1007/s13127-011-0056-0>
- Sindaco, R. & Jeremčenko, V.K. (2008) *The reptiles of the Western Palearctic. Annotated checklist and distributional atlas of the turtles, crocodiles, amphisbaenians and lizards of Europe, North Africa, Middle East and Central Asia*. Monografie della Societas Herpetologica Italica. Edizioni Belvedere, Latina, 579 pp.
- Stamatakis, A. (2006) RAXML-VI-HP: maximum likelihood-based phylogenetic analyses with thousands of taxa and mixed models. *Bioinformatics*, 22, 2688–2690.
<https://doi.org/10.1093/bioinformatics/btl446>
- Stamatakis, A., Hoover, P. & Rougemont, J. (2008) A rapid bootstrap algorithm for the RAXML web servers. *Systematic Biology*, 57, 758–771.
<https://doi.org/10.1080/10635150802429642>
- Stephens, M. & Scheet, P. (2005) Accounting for decay of linkage disequilibrium in haplotype inference and missing-data imputation. *The American Journal of Human Genetics*, 76.3, 449–462.
<https://doi.org/10.1086/428594>
- Stephens, M., Smith, N.J. & Donnelly, P. (2001) A new statistical method for haplotype reconstruction from population data. *The American Journal of Human Genetics*, 68, 978–989.
<https://doi.org/10.1086/319501>
- Talavera, G. & Castresana, J. (2007) Improvement of phylogenies after removing divergent and ambiguously aligned blocks from protein sequence alignments. *Systematic Biology*, 56, 564–577.
<https://doi.org/10.1080/10635150701472164>
- Tamar, K., Carranza, S., Sindaco, R., Moravec, J. & Meiri, S. (2014) Systematics and phylogeography of *Acanthodactylus schreiberi* and its relationships with *Acanthodactylus boskianus* (Reptilia: Squamata: Lacertidae). *Zoological Journal of the Linnean Society*, 172, 720–739.
<https://doi.org/10.1111/zoj.12170>
- Tamar, K., Carranza, S., Sindaco, R., Moravec, J., Trape, J.-F. & Meiri, S. (2016) Out of Africa: Phylogeny and biogeography of the widespread genus *Acanthodactylus* (Reptilia: Lacertidae). *Molecular Phylogenetics and Evolution*, 103, 6–18.
<https://doi.org/10.1016/j.ympev.2016.07.003>
- Trape, J.-F., Trape, S. & Chirio, L. (2012) *Lézards, crocodiles et tortues d'Afrique occidentale et du Sahara*. IRD Orstom, Marseille, 503 pp.
- Uetz, P. & Hošek, J. (2017) The Reptile Database. Available from: <http://www.reptile-database.org> (accessed 25 March 2017)
- Wilcox, T.P., Zwickl, D.J., Heath, T.A. & Hillis, D.M. (2002) Phylogenetic relationships of the dwarf boas and a comparison of Bayesian and bootstrap measures of phylogenetic support. *Molecular Biology and Evolution*, 25, 361–371.
[https://doi.org/10.1016/S1055-7903\(02\)00244-0](https://doi.org/10.1016/S1055-7903(02)00244-0)

APPENDIX I. Data on the *pardalis* species-group members (excluding *A. busacki* and *A. margaritae* sp. nov.), used in the genetic analyses, with specimen codes, localities and related GenBank accession codes (from Tamar *et al.* 2016).

Specimen code	Tentative identification	Country	Locality	12S	cytb	MCIr	ACM4	c-mos
A258	<i>A. bedriagai</i>	Algeria	Djelfa	KX296941	KX297144	KX297325	KX297447	KX297647
A189	<i>A. bedriagai</i>	Tunisia	Roman Ruins Bou Chebka-Haidra	KX296948	KX297153	KX297346	KX297446	KX297628
A283	<i>A. beershebensis</i>	Israel	3 km S. of Ofakim	KX296956	KX297158	KX297327	KX297451	KX297620
A75	<i>A. beershebensis</i>	Israel	3 km S. of Ofakim	KX296958	KX297159	-	-	-
A280	<i>A. beershebensis</i>	Israel	E. to park Arad	KX296954	KX297156	-	-	-
A74	<i>A. beershebensis</i>	Israel	E. to park Arad	KX296955	KX297157	KX297328	KX297452	KX297621
A40	<i>A. beershebensis</i>	Israel	Hanegev junction	KX296961	KX297164	-	KX297449	KX297617
A53	<i>A. beershebensis</i>	Israel	Hanegev junction	KX296963	KX297166	KX297326	KX297450	KX297619
A17	<i>A. beershebensis</i>	Israel	Nahal Hed	KX296960	KX297163	KX297342	KX297453	KX297622
A2	<i>A. beershebensis</i>	Israel	Nahal Hed	KX296959	KX297161	KX297329	KX297456	KX297616
A47	<i>A. beershebensis</i>	Israel	Nahal Hed	KX296962	KX297165	KX297330	KX297455	KX297618
A278	<i>A. beershebensis</i>	Israel	Nahal Tzavoa	KX296964	KX297160	-	-	-
A284	<i>A. beershebensis</i>	Israel	NW. to road 40	KX296957	KX297162	-	-	-
A141	<i>A. maculatus</i>	Algeria	Al Aricha	KX296937	KX297137	KX297323	KX297427	KX297615
A142	<i>A. maculatus</i>	Algeria	Al Aricha	KX296938	KX297138	KX297324	KX297428	KX297623
A259	<i>A. maculatus</i>	Algeria	25 km SE. of El Bayadh	KX296942	KX297145	KX297351	KX297448	KX297643
A91	<i>A. maculatus</i>	Libya	5 km E. of Al Jawsh	KX296951	KX297142	KX297341	KX297458	KX297625
A58	<i>A. maculatus</i>	Morocco	6 km N. of Erfoud	KX296952	KX297149	KX297353	KX297457	KX297634
A143	<i>A. maculatus</i>	Morocco	El Aioun	KX296940	KX297143	KX297340	KX297442	KX297649
A262	<i>A. maculatus</i>	Morocco	North shore of Dayet Srtji (near Merzouga)	KX296953	KX297150	-	-	KX297635
A49	<i>A. maculatus</i>	Morocco	10 km N. of Midelt	KX296944	KX297147	KX297352	KX297443	KX297631
A52	<i>A. maculatus</i>	Morocco	3 km N. of Boulojou	KX296945	KX297148	KX297343	KX297444	KX297632
A90	<i>A. maculatus</i>	Morocco	Tafraata plain	KX296943	KX297146	-	-	KX297633
A144	<i>A. maculatus</i>	Tunisia	Close to Kasserine	KX296946	KX297151	KX297345	KX297429	KX297640

..... continued on the next page

APPENDIX 1. (Continued)

Specimen code	Tentative identification	Country	Locality	12S	cytb	MCIR	ACM4	c-mos
A145	<i>A. maculatus</i>	Tunisia	Close to Kasserine	KX296947	KX297152	KX297347	KX297445	KX297648
A81	<i>A. maculatus</i>	Tunisia	Sidi Mechrig	KX296949	KX297154	KX297333	KX297438	KX297641
A82	<i>A. maculatus</i>	Tunisia	Sidi Mechrig	KX296950	KX297155	KX297334	KX297439	KX297642
MB03-879	<i>A. maculatus</i>	Morocco	15km S. of Saka	KY807723	KY807732	KY807741	KY807749	KY807757
MB03-880	<i>A. maculatus</i>	Morocco	15km S. of Saka	KY807724	KY807733	-	KY807750	KY807758
MB03-883	<i>A. maculatus</i>	Libya	Hamadath al Hamrah; 172 km SE. of Derj	KY807725	KY807734	KY807742	KY807751	KY807759
MB03-884	<i>A. maculatus</i>	Libya	Hamadath al Hamrah; 172 km SE. of Derj	KY807726	KY807735	KY807743	-	KY807760
A227	<i>A. pardalis</i>	Egypt	---	KX296934	-	-	-	-
A41	<i>A. pardalis</i>	Egypt	El Nasr	KX296935	KX297139	KX297344	KX297440	KX297637
A54	<i>A. pardalis</i>	Egypt	El Nasr	KX296936	KX297141	KX297335	KX297454	KX297639
A55	<i>A. pardalis</i>	Egypt	El Nasr	KX296939	KX297140	KX297331	KX297441	KX297638
A126	<i>A. erythrurus</i>	Spain	Darrical	KX296925	KX297128	KX297315	KX297419	KX297602
A125	<i>A. erythrurus</i>	Spain	Barbate	KX296928	KX297127	KX297312	KX297408	KX297601

APPENDIX II. *Acanthodactylus* specimens used for the morphological examination with localities and data collection type (for voucher specimens - voucher specimen examined or only photographs of the specimen examined; photographic material of specimens in nature was used for meristic characters and colouration). Taxon names follow the taxonomy recommended in this study. Coordinates (WGS84, decimal degrees) are given with two decimals for coordinates deduced from the locality description and three to four decimals for coordinates that provide more precise location than the locality itself (for example obtained in the field with a GPS). Specimen code abbreviations: [BEV] Biogéographie et Écologie des Vertébrés, Centre d'Écologie Fonctionnelle et Évolutive, Montpellier, France; [BMNH] Natural History Museum, London, England; [CAS] California Academy of Sciences, San Francisco, USA; [FMNH] Field Museum of Natural History, Chicago, USA; [MB] Museu Nacional de História Natural e da Ciência (MUHNAC), Lisbon, Portugal; [MCCI-R] Museo Civico di Storia Naturale, Carmagnola, Turin, Italy; [MNHN-P] Muséum national d'Histoire naturelle, Paris, France; [PGE] Photo collection of Philippe Geniez, Montpellier, France; [ZFMK] Zoologisches Forschungsmuseum Alexander Koenig, Bonn, Germany; [ZMH] Zoologisches Museum Hamburg, Germany.

Specimen code	Species	Country	Locality	Latitude	Longitude	Data type
BEV.5498	<i>A. margaritae</i> sp. nov.	Morocco	Agadir-Taroudant road, Biougra, Ademine forest	30.32	-9.36	Voucher Specimen
BEV.5504	<i>A. margaritae</i> sp. nov.	Morocco	1 km E. of Atlantic Ocean, north bank of Oued Massa	30.0740	-9.6660	Voucher Specimen
BEV.5505	<i>A. margaritae</i> sp. nov.	Morocco	1 km E. of Atlantic Ocean, north bank of Oued Massa	30.0740	-9.6660	Voucher Specimen
BEV.9440	<i>A. margaritae</i> sp. nov.	Morocco	1.6 km S. of Agadir-Taroudant new road towards Biougra, Ademine forest	30.3158	-9.3600	Voucher Specimen
MCCI-R.560	<i>A. margaritae</i> sp. nov. Paratype	Morocco	Between Inchaden and Tifinite	30.15	-9.59	Voucher Specimen
MCCI-R.561	<i>A. margaritae</i> sp. nov. Paratype	Morocco	Souss valley, Outskirts of Biougra	30.21	-9.38	Voucher Specimen
MCCI-R.562	<i>A. margaritae</i> sp. nov. Paratype	Morocco	Souss valley, Outskirts of Biougra	30.21	-9.38	Voucher Specimen
MNHN-RA-2016.0105	<i>A. margaritae</i> sp. nov. Holotype	Morocco	Massa park, slopes above the Sidi R'bat park entrance, near Sidi Binzarne	30.0580	-9.6456	Voucher Specimen
ZFMK 16068	<i>A. margaritae</i> sp. nov.	Morocco	10 km S. of Taroudannt	30.38	-8.87	Voucher Specimen
ZFMK 16069	<i>A. margaritae</i> sp. nov.	Morocco	10 km S. of Taroudannt	30.38	-8.87	Voucher Specimen
ZFMK 16071	<i>A. margaritae</i> sp. nov.	Morocco	10 km S. of Taroudannt	30.38	-8.87	Voucher Specimen
ZFMK 16072	<i>A. margaritae</i> sp. nov.	Morocco	10 km S. of Taroudannt	30.38	-8.87	Voucher Specimen
ZFMK 16073	<i>A. margaritae</i> sp. nov.	Morocco	10 km S. of Taroudannt	30.38	-8.87	Voucher Specimen
ZFMK 16076	<i>A. margaritae</i> sp. nov.	Morocco	Agadir	30.42	-9.59	Voucher Specimen
ZFMK 16077	<i>A. margaritae</i> sp. nov.	Morocco	Agadir	30.42	-9.59	Voucher Specimen
ZFMK 18869	<i>A. margaritae</i> sp. nov.	Morocco	Inezgane, Agadir	30.34	-9.56	Voucher Specimen
ZFMK 25826	<i>A. margaritae</i> sp. nov.	Morocco	Outskirts of Agadir	30.40	-9.50	Voucher Specimen
ZFMK 25827	<i>A. margaritae</i> sp. nov.	Morocco	Outskirts of Agadir	30.40	-9.50	Voucher Specimen
ZFMK 25830	<i>A. margaritae</i> sp. nov.	Morocco	Outskirts of Agadir	30.40	-9.50	Voucher Specimen
ZFMK 25832	<i>A. margaritae</i> sp. nov.	Morocco	Outskirts of Agadir	30.40	-9.50	Voucher Specimen
ZFMK 25833	<i>A. margaritae</i> sp. nov.	Morocco	Outskirts of Agadir	30.40	-9.50	Voucher Specimen
ZFMK 25834	<i>A. margaritae</i> sp. nov.	Morocco	Outskirts of Agadir	30.40	-9.50	Voucher Specimen
ZFMK 25835	<i>A. margaritae</i> sp. nov.	Morocco	Outskirts of Agadir	30.40	-9.50	Voucher Specimen

.....continued on the next page

APPENDIX II. (Continued)

Specimen code	Species	Country	Locality	Latitude	Longitude	Data type
ZFMK 25836	<i>A. margaritae</i> sp. nov.	Morocco	Outskirts of Agadir	30.40	-9.50	Voucher Specimen
ZFMK 25837	<i>A. margaritae</i> sp. nov.	Morocco	Outskirts of Agadir	30.40	-9.50	Voucher Specimen
ZFMK 25838	<i>A. margaritae</i> sp. nov.	Morocco	Outskirts of Agadir	30.40	-9.50	Voucher Specimen
ZFMK 25840	<i>A. margaritae</i> sp. nov.	Morocco	Outskirts of Agadir	30.40	-9.50	Voucher Specimen
ZFMK 25841	<i>A. margaritae</i> sp. nov.	Morocco	Outskirts of Agadir	30.40	-9.50	Voucher Specimen
ZFMK 44064	<i>A. margaritae</i> sp. nov.	Morocco	6 km S. of Taroudant	30.42	-8.88	Voucher Specimen
ZFMK 44065	<i>A. margaritae</i> sp. nov.	Morocco	7 km S. of Taroudant	30.41	-8.88	Voucher Specimen
ZFMK 73027	<i>A. margaritae</i> sp. nov.	Morocco	Outskirts of Agadir	30.40	-9.50	Voucher Specimen
ZFMK 73028	<i>A. margaritae</i> sp. nov.	Morocco	Outskirts of Agadir	30.40	-9.50	Voucher Specimen
ZFMK 73029	<i>A. margaritae</i> sp. nov.	Morocco	Outskirts of Agadir	30.40	-9.50	Voucher Specimen
ZFMK 79410	<i>A. margaritae</i> sp. nov.	Morocco	Cap Ghir (= Rhir)	30.63	-9.89	Voucher Specimen
ZFMK 79411	<i>A. margaritae</i> sp. nov.	Morocco	Tifite	30.20	-9.64	Voucher Specimen
ZFMK 79412	<i>A. margaritae</i> sp. nov.	Morocco	Tifite	30.20	-9.64	Voucher Specimen
ZFMK 79413	<i>A. margaritae</i> sp. nov.	Morocco	Tifite	30.20	-9.64	Voucher Specimen
ZFMK 79414	<i>A. margaritae</i> sp. nov.	Morocco	Tifite	30.20	-9.64	Voucher Specimen
BMNH 1970.246	<i>A. margaritae</i> sp. nov.	Morocco	N. of Agadir	30.52	-9.68	Voucher Photograph
BMNH 1970.247	<i>A. margaritae</i> sp. nov.	Morocco	N. of Agadir	30.52	-9.68	Voucher Photograph
BMNH 1970.248	<i>A. margaritae</i> sp. nov.	Morocco	20 km N. of Tiznit	29.87	-9.72	Voucher Photograph
CAS 92450	<i>A. margaritae</i> sp. nov.	Morocco	Shores of Oued Souss near Taroudant	30.45	-8.88	Voucher Photograph
CAS 92451	<i>A. margaritae</i> sp. nov.	Morocco	Shores of Oued Souss near Taroudant	30.45	-8.88	Voucher Photograph
MB03-887	<i>A. margaritae</i> sp. nov.	Morocco	1 km E. of Atlantic Ocean, W. of Tamellalt	29.8061	-9.6475	Voucher Photograph
MB03-888	<i>A. margaritae</i> sp. nov.	Morocco	1 km E. of Atlantic Ocean, W. of Tamellalt	29.8061	-9.6475	Voucher Photograph
MB03-889	<i>A. margaritae</i> sp. nov.	Morocco	1 km E. of Atlantic Ocean, W. of Tamellalt	29.8061	-9.6475	Voucher Photograph
MB03-890	<i>A. margaritae</i> sp. nov.	Morocco	1 km E. of Atlantic Ocean, W. of Tamellalt	29.8061	-9.6475	Voucher Photograph
MB03-891	<i>A. margaritae</i> sp. nov.	Morocco	1 km E. of Atlantic Ocean, W. of Tamellalt	29.8061	-9.6475	Voucher Photograph
MB03-892	<i>A. margaritae</i> sp. nov.	Morocco	1 km E. of Atlantic Ocean, W. of Tamellalt	29.8061	-9.6475	Voucher Photograph
FMNH 197897	<i>A. margaritae</i> sp. nov.	Morocco	9 km N. of Tamri	30.77	-9.82	Voucher Photograph
FMNH 197898	<i>A. margaritae</i> sp. nov.	Morocco	9 km N. of Tamri	30.77	-9.82	Voucher Photograph
FMNH 199916	<i>A. margaritae</i> sp. nov.	Morocco	Agadir province			Voucher Photograph
FMNH 199917	<i>A. margaritae</i> sp. nov.	Morocco	Agadir province			Voucher Photograph
FMNH 199919	<i>A. margaritae</i> sp. nov.	Morocco	Agadir province			Voucher Photograph

.....continued on the next page

APPENDIX II. (Continued)

Specimen code	Species	Country	Locality	Latitude	Longitude	Data type
FMNH 199920	<i>A. margaritae</i> sp. nov.	Morocco	Agadir province			Voucher Photograph
FMNH 199921	<i>A. margaritae</i> sp. nov.	Morocco	Agadir province			Voucher Photograph
ZMH 04305	<i>A. margaritae</i> sp. nov.	Morocco	Outskirts of Agadir	30.40	-9.50	Voucher Photograph
PGe.145	<i>A. margaritae</i> sp. nov.	Morocco	Wadi between Sidi Moussa Lhamri and Labaarir	30.4727	-9.1415	Photograph
PGe.146	<i>A. margaritae</i> sp. nov.	Morocco	Wadi between Sidi Moussa Lhamri and Labaarir	30.4727	-9.1415	Photograph
PGe.147	<i>A. margaritae</i> sp. nov.	Morocco	Forestry house of Ademine, 4 km E. of Ikhourbane	30.33	-9.37	Photograph
PGe.148	<i>A. margaritae</i> sp. nov.	Morocco	2 km E. of Sidi R'Bat	30.0808	-9.6484	Photograph
PGe.149	<i>A. margaritae</i> sp. nov.	Morocco	Wadi, 8 km N. of Tamri	30.7652	-9.8215	Photograph
PGe.150	<i>A. margaritae</i> sp. nov.	Morocco	16 km from the Taroudant-Ouarzazate road towards Igherm	30.4099	-8.6203	Photograph
PGe.151	<i>A. margaritae</i> sp. nov.	Morocco	3 km NE. of Sidi Boulfdail	29.6997	-9.9405	Photograph
PGe.152	<i>A. margaritae</i> sp. nov.	Morocco	3 km NE. of Sidi Boulfdail	29.6997	-9.9405	Photograph
PGe.153	<i>A. margaritae</i> sp. nov.	Morocco	Village of Sidi Ouassay (near Massa)	30.057	-9.683	Photograph
PGe.158	<i>A. margaritae</i> sp. nov.	Morocco	9 km E. of Oulad Teima	30.412	-9.125	Photograph
PGe.159	<i>A. margaritae</i> sp. nov.	Morocco	7 km E. of Oulad Teima	30.412	-9.151	Photograph
PGe.1139	<i>A. margaritae</i> sp. nov.	Morocco	9 km N. of Tiznit	29.78	-9.68	Photograph
PGe.1140	<i>A. margaritae</i> sp. nov.	Morocco	Belfaa (S. of Agadir)	30.049	-9.566	Photograph
PGe.1141	<i>A. margaritae</i> sp. nov.	Morocco	Belfaa (S. of Agadir)	30.049	-9.566	Photograph
PGe.1142	<i>A. margaritae</i> sp. nov.	Morocco	Forestry house of Ademine, 4 km E. of Ikhourbane	30.33	-9.37	Photograph
PGe.1143	<i>A. margaritae</i> sp. nov.	Morocco	Aglou-Plage	29.806	-9.827	Photograph
PGe.1144	<i>A. margaritae</i> sp. nov.	Morocco	Between Sidi R'bat and the river Oued Massa	30.083	-9.667	Photograph
PGe.1145	<i>A. margaritae</i> sp. nov.	Morocco	400 m E. of Atlantic Ocean, Asif n'Srou river estuary	30.7093	-9.8540	Photograph
PGe.1146	<i>A. margaritae</i> sp. nov.	Morocco	Shore of Atlantic Ocean, Asif n'Srou river estuary	30.7095	-9.8571	Photograph
PGe.1147	<i>A. margaritae</i> sp. nov.	Morocco	Dunes, 1 km N. of Asif n'Srou river estuary	30.719	-9.849	Photograph
PGe.1148	<i>A. margaritae</i> sp. nov.	Morocco	Near cliffs, 1 km S. of Asif n'Srou river estuary	30.702	-9.866	Photograph
PGe.1170	<i>A. margaritae</i> sp. nov.	Morocco	Sidi Toual (S. of Agadir)	30.278	-9.612	Photograph
PGe.1171	<i>A. margaritae</i> sp. nov.	Morocco	Sidi Toual (S. of Agadir)	30.278	-9.612	Photograph
PGe.1172	<i>A. margaritae</i> sp. nov.	Morocco	Souss Massa Park	30.08	-9.65	Photograph
PGe.1173	<i>A. margaritae</i> sp. nov.	Morocco	10 km NE. of Tiznit	29.767	-9.669	Photograph
PGe.1174	<i>A. margaritae</i> sp. nov.	Morocco	0.5 km N. of Zaouite Aglou, wadi Oudoudou	29.799	-9.808	Photograph
PGe.1175	<i>A. margaritae</i> sp. nov.	Morocco	0.5 km N. of Zaouite Aglou, wadi Oudoudou	29.799	-9.808	Photograph
PGe.1176	<i>A. margaritae</i> sp. nov.	Morocco	500 m NW. of Sidi Binzarne, east bank of Oued Massa	30.0578	-9.6558	Photograph

.....continued on the next page

APPENDIX II. (Continued)

Specimen code	Species	Country	Locality	Latitude	Longitude	Data type
PGe.1177	<i>A. margaritae</i> sp. nov.	Morocco	1 km E. of Atlantic Ocean, east bank of Oued Massa	30.0745	-9.6669	Photograph
BEV.5499	<i>A. busacki</i>	Morocco	7 km W. of Tantan towards El-Ouatia	28.467	-11.165	Voucher Specimen
BEV.5506	<i>A. busacki</i>	Morocco	Hassi Zehar	27.957	-11.946	Voucher Specimen
BEV.5507	<i>A. busacki</i>	Morocco	Hassi Zehar	27.957	-11.946	Voucher Specimen
BEV.5508	<i>A. busacki</i>	Morocco	Hassi Zehar	27.957	-11.946	Voucher Specimen
BEV.10466	<i>A. busacki</i>	Morocco	Between Laayoune and Boujdour, 5 km NE. of Lamsid	26.5671	-13.7923	Voucher Specimen
BEV.10829	<i>A. busacki</i>	Morocco	Vegetated wadi N. of Akhfennir	28.1001	-12.0389	Voucher Specimen
BEV.10869	<i>A. busacki</i>	Morocco	Tarfaya road - El Watan El Ouatia	28.2656	-11.5908	Voucher Specimen
BEV.10877	<i>A. busacki</i>	Morocco	Dakhla - Boujdour road, 104 km NNW. of Dakhla	24.3898	-15.2494	Voucher Specimen
BEV.11435	<i>A. busacki</i>	Morocco	Cape Boujdour	26.127	-14.499	Voucher Specimen
BEV.11436	<i>A. busacki</i>	Morocco	Cape Boujdour	26.127	-14.499	Voucher Specimen
MNHN-RA-1938.189	<i>A. busacki</i> Paratype	Morocco	Asrifa, 26°19'N/13°42'	26.32	-13.70	Voucher Specimen
BMNH 1970.250	<i>A. busacki</i> Holotype	Morocco	30 km SW. of Goulimine (=Guelmin)	28.82	-10.28	Voucher Photograph
MB03-886	<i>A. busacki</i>	Morocco	Road Tarfaya - Laayoune, 10 km SSW. of Tah	27.5956	-12.9984	Voucher Photograph
PGe.154	<i>A. busacki</i>	Morocco	8 km W. of Tantan towards El-Ouatia	28.468	-11.174	Photograph
PGe.155	<i>A. busacki</i>	Morocco	Tantan - Abateh road, 21 km S. of Tantan	28.293	-11.194	Photograph
PGe.156	<i>A. busacki</i>	Morocco	Abateh - Smara road, 44 km S. of Abateh, N. boundary of Smara province	27.571	-11.636	Photograph
PGe.157	<i>A. busacki</i>	Morocco	Abateh - Smara road, 44 km S. of Abateh, N. boundary of Smara province	27.571	-11.636	Photograph
PGe.1149	<i>A. busacki</i>	Morocco	South-west of Garet Es-Souf, 13 km SW. of Sidi Akhfennir	27.9835	-12.0959	Photograph
PGe.1150	<i>A. busacki</i>	Morocco	NE. of Boujdour	26.25	-14.39	Photograph
PGe.1151	<i>A. busacki</i>	Morocco	21 km SE. of Khmifiss	27.92	-12.07	Photograph
PGe.1152	<i>A. busacki</i>	Morocco	Outskirts of Tantan	28.45	-11.11	Photograph
PGe.1153	<i>A. busacki</i>	Morocco	Outskirts of Tantan	28.45	-11.11	Photograph
PGe.1154	<i>A. busacki</i>	Morocco	Outskirts of Tantan	28.45	-11.11	Photograph
PGe.1155	<i>A. busacki</i>	Morocco	36 km SE. of Sidi Akhfennir, 27°49'N-11°51'W	27.82	-11.85	Photograph
PGe.1156	<i>A. busacki</i>	Morocco	Between Tafnildit and Guelmim, 2 km N. of Zhiouila	28.843	-10.236	Photograph
PGe.1157	<i>A. busacki</i>	Morocco	Guelmim - Tantan road, 5 km S. of Labyar	28.792	-10.426	Photograph
PGe.1158	<i>A. busacki</i>	Morocco	Guelmim - Tantan road, 4 km SE. of Labyar	28.82	-10.39	Photograph
PGe.1159	<i>A. busacki</i>	Morocco	Guelmim-Tantan road, 4 km E. of Nofia	28.628	-10.765	Photograph
PGe.1160	<i>A. busacki</i>	Morocco	6 km SW. of Daoura	27.4213	-13.0283	Photograph

.....continued on the next page

APPENDIX II. (Continued)

Specimen code	Species	Country	Locality	Latitude	Longitude	Data type
PGe.1161	<i>A. busacki</i>	Morocco	6 km SW. of Daoura	27.4213	-13.0283	Photograph
PGe.1162	<i>A. busacki</i>	Morocco	6 km SW. of Daoura	27.4213	-13.0283	Photograph
PGe.1163	<i>A. busacki</i>	Morocco	7 km ENE. of Boujdour	26.1551	-14.4190	Photograph
PGe.1164	<i>A. busacki</i>	Morocco	7 km ENE. of Boujdour	26.1551	-14.4190	Photograph
PGe.1165	<i>A. busacki</i>	Morocco	7 km ENE. of Boujdour	26.1551	-14.4190	Photograph
PGe.1166	<i>A. busacki</i>	Morocco	7 km ENE. of Boujdour	26.1551	-14.4190	Photograph
PGe.1167	<i>A. busacki</i>	Morocco	Outskirts of Tantan	28.45	-11.11	Photograph
PGe.1168	<i>A. busacki</i>	Morocco	Outskirts of Tantan	28.45	-11.11	Photograph
PGe.1169	<i>A. busacki</i>	Morocco	16 km W. of Tantan, direction of El-Ouatia	28.474	-11.236	Photograph
MNHN-RA-1925.175	<i>A. cf. maculatus</i>	Morocco	Mahirija	33.99	-3.28	Voucher Specimen
MNHN-RA-1925.176	<i>A. cf. maculatus</i>	Morocco	Mahirija	33.99	-3.28	Voucher Specimen
MNHN-RA-1925.178	<i>A. cf. maculatus</i>	Morocco	Taurirt	34.42	-2.90	Voucher Specimen
MNHN-RA-1925.179	<i>A. cf. maculatus</i>	Morocco	Taurirt	34.42	-2.90	Voucher Specimen
MNHN-RA-1925.180	<i>A. cf. maculatus</i>	Morocco	Taurirt	34.42	-2.90	Voucher Specimen
MNHN-RA-1925.181	<i>A. cf. maculatus</i>	Morocco	Taurirt	34.42	-2.90	Voucher Specimen
MNHN-RA-1925.182	<i>A. cf. maculatus</i>	Morocco	Taurirt	34.42	-2.90	Voucher Specimen
MNHN-RA-1925.183	<i>A. cf. maculatus</i>	Morocco	Taurirt	34.42	-2.90	Voucher Specimen
MNHN-RA-1925.184	<i>A. cf. maculatus</i>	Morocco	Itzer	32.88	-5.05	Voucher Specimen
MNHN-RA-1925.185	<i>A. cf. maculatus</i>	Morocco	Itzer	32.88	-5.05	Voucher Specimen
MNHN-RA-1925.186	<i>A. cf. maculatus</i>	Morocco	Itzer	32.88	-5.05	Voucher Specimen
MNHN-RA-1925.187	<i>A. cf. maculatus</i>	Morocco	Itzer	32.88	-5.05	Voucher Specimen
MNHN-RA-1925.188	<i>A. cf. maculatus</i>	Morocco	Itzer	32.88	-5.05	Voucher Specimen
MNHN-RA-1925.189	<i>A. cf. maculatus</i>	Morocco	Itzer	32.88	-5.05	Voucher Specimen
MNHN-RA-1925.190	<i>A. cf. maculatus</i>	Morocco	Itzer	32.88	-5.05	Voucher Specimen
MNHN-RA-1925.192	<i>A. cf. maculatus</i>	Morocco	Ain Guettara	33.90	-3.40	Voucher Specimen
MNHN-RA-1925.193	<i>A. cf. maculatus</i>	Morocco	Ain Guettara	33.90	-3.40	Voucher Specimen
MNHN-RA-1927.122	<i>A. cf. maculatus</i>	Morocco	Ain Guettara	33.90	-3.40	Voucher Specimen
MB03-878	<i>A. cf. maculatus</i>	Morocco	30km N. of Missour	33.2654	-3.8040	Voucher Photograph
MB03-879	<i>A. cf. maculatus</i>	Morocco	15km S. of Saka	34.4967	-3.3261	Voucher Photograph
MB03-880	<i>A. cf. maculatus</i>	Morocco	15km S. of Saka	34.4967	-3.3261	Voucher Photograph
MB03-881	<i>A. cf. maculatus</i>	Morocco	15km S. of Saka	34.4967	-3.3261	Voucher Photograph
MB03-882	<i>A. cf. maculatus</i>	Morocco	10 km N. of El Aioun	34.6444	-2.4411	Voucher Photograph

APPENDIX III. Maximum likelihood phylogenetic tree of the *pardalis* species-group reconstructed from 2405 bp of mitochondrial (*12S*, *cytb*) and nuclear (*MC1R*, *ACM4*, *c-mos*) gene fragments. Bootstrap and posterior probabilities values are presented near the nodes (ML/BI; values $\geq 70\%$ and ≥ 0.95 , respectively). Taxon names correspond to changes proposed in this paper.

